8-24-2010

A Role for Cilia in Endocardial Cushion Development

Laura Gilbert Hollingsworth Cooney
Yale University

A Role for Cilia in Endocardial Cushion Development

A Thesis Submitted to the

Yale University School of Medicine

In Partial Fulfillment of the Requirements for the

Degree of Doctor of Medicine

By

Laura Gilbert Hollingsworth Cooney

2010

Abstract

A Role for Cilia in Endocardial Cushion Development

Laura Cooney, Jennifer Slough, Martina Brueckner

Department of Pediatrics and Genetics, Yale University School of Medicine,

New Haven, CT

Congenital heart defects due to the aberrant development of the atrioventricular (AV) valves and septum are among the most common developmental abnormality in newborns and cause significant neonatal morbidity and mortality. A key point in cardiac morphogenesis occurs when cells within the endocardial cushions (ECCs), the precursors for the AV valvoseptal complex, delaminate and undergo an epithelial-to-mesenchymal transformation (EMT). The mesenchymal cells then proliferate and the cushion area elongates to form the AV valves and portions of the AV septae. The signals that initiate region-specific EMT during heart development are unknown. Cilia, known for their role in establishing left-right (LR) asymmetry, function to receive and integrate extracellular signals, including fluid flow, in a range of other organ systems. We hypothesize that cilia could also have a direct role in heart development outside of their role in LR development. Using immunohistochemistry, we demonstrated the presence of cilia on the myocardium, epicardium, and ECCs of wild-type mouse hearts at embryonic day (e) 9.5 and e12.5. To characterize the potential role of these cilia, we compared mice with mutations affecting ciliary biogenesis, motility, and mechanosensation. Using bright field microscopy and *in situ* hybridization, we analyzed the embryonic heart structure and the expression pattern of Gata4, an EMT transcription factor. We showed that compared

to mice with immotile but structurally normal cilia, the mice without cilia had hypocellular ECCs, a thinned compact myocardium (CM), and an up-regulated expression of Gata4. These observations suggest that a subset of cilia called *cardiac cilia* have a role in cardiogenesis outside of their role in LR development and affect Gata4 expression. One possible function of cardiac cilia is as mechanosensors, integrating fluid flow and influencing cardiac morphogenesis including EMT and development of the CM.

Acknowledgements

I would first like to thank my mentor, Dr. Martina Brueckner, for instilling in me an appreciation and excitement for the complex world of cilia and heart development. With her help, I was able to go beyond the initial frustrating days when my *in situ* hybridizations did not work and to experience the feelings of success at gazing under a microscope and seeing the heart light up with my probes. Thank you for your support and instruction.

I would also like to thank my other lab members. First, thanks to Jennifer Slough for teaching me each technique and for her help in completing some of the experiments mentioned in this thesis. Thanks to Svetlana Makova for her friendship and her endless patience in answering my questions and to Jeffrey Drozd for his instruction in handling and genotyping mice.

I would like to thank my parents, Jeanne and Scott, for supporting me through all of my medical school endeavors. Finally, I would like to thank my husband, Patrick, for his understanding during my late night trips to the lab, his kind words when some my experiments were not working as planned, and his patient proofreading of all of my manuscripts.

Table of Contents

Introduction

Congenital heart defects are the most common developmental abnormality in newborns, affecting 4-6 infants for every 1000 live births (1). A significant portion of these cardiovascular malformations arises from aberrant development of the atrioventricular (AV) valves and septum. These defects can be associated with genetic syndromes such as Trisomies 16, 18, and 21 or Noonan syndrome. However, as many as 25% of patients with defects in the endocardial cushions (ECCs), the precursors for the AV valvoseptal complex, do not have a defined genetic syndrome (1). Although much is understood about the genetic and epigenetic contributions to valvular and septal morphogenesis, the complete developmental pathway has yet to be elucidated. Because cardiovascular defects are a large cause of infant morbidity and mortality, there is significant interest in understanding the mechanisms that contribute to this developmental process.

1. Heart Development is a Complex Process Coordinated by Different Cell Types and Signaling Pathways.

1a. Overview of Heart Development

The mammalian heart is the first organ to form during embryogenesis and begins to function even before it is fully developed. Heart morphogenesis is supported by a complex series of carefully related processes which ultimately create a muscular four-chambered pump capable of supplying blood to the entire body. During gastrulation, cells in the anterior primitive streak are specified to be cardiac progenitor cells. After first migrating anteriorly and laterally, these cells fuse to form a linear heart tube (2,3).

At mouse embryonic day (e) 8.0-8.25 this early straight heart tube consists of an outer myocardial layer separated from an inner endocardial cell layer by an extracellular matrix (ECM) called the cardiac jelly (Fig. 1A). Around e8.5, the primary linear heart transforms into a helically wound heart loop in a morphogenic process called cardiac looping, in which the ventricular portion begins to curve to the right (Fig. 1B). This process sets up the basic topographical left-right (LR) asymmetry as well as brings the atrial regions in proximity to the ventricular regions in preparation for forming four separate chambers (4). It is at this point that myocardial cells enhance the secretion of ECM in the outflow tract (OFT) and at junctions between the atrium and left ventricle (Fig. 1C). These regions of cardiac jelly hypertrophy, called endocardial cushions (ECCs), consist of glycosaminoglycans such as hyaluronic acid (HA), a hydrophilic molecule that promotes swelling of the acellular space. The ECCs subsequently undergo significant differentiation and growth and by e12.5 begin extensive remodeling to form the aortic, pulmonic, tricuspid, and mitral valves as well as the AV septum (2,3).

1b. An Epithelial to Mesenchymal Transformation in the Endocardial Cushions Underlies Valve and Septum Development

Substantial progress has been made in elucidating the complex process through which the ECCs develop into the AV valvoseptal complex. Early observations of mesenchymal cells (Fig. 1D) in the ECCs of Hamburger and Hamilton (HH) stage 17-18 chickens prompted speculation as to whether these cells developed from the myocardial or endocardial cell layer (5,6). In studies using time-lapse microscopy of cultured AV canals, endocardial cells were observed to extend filapodia, detach from neighboring

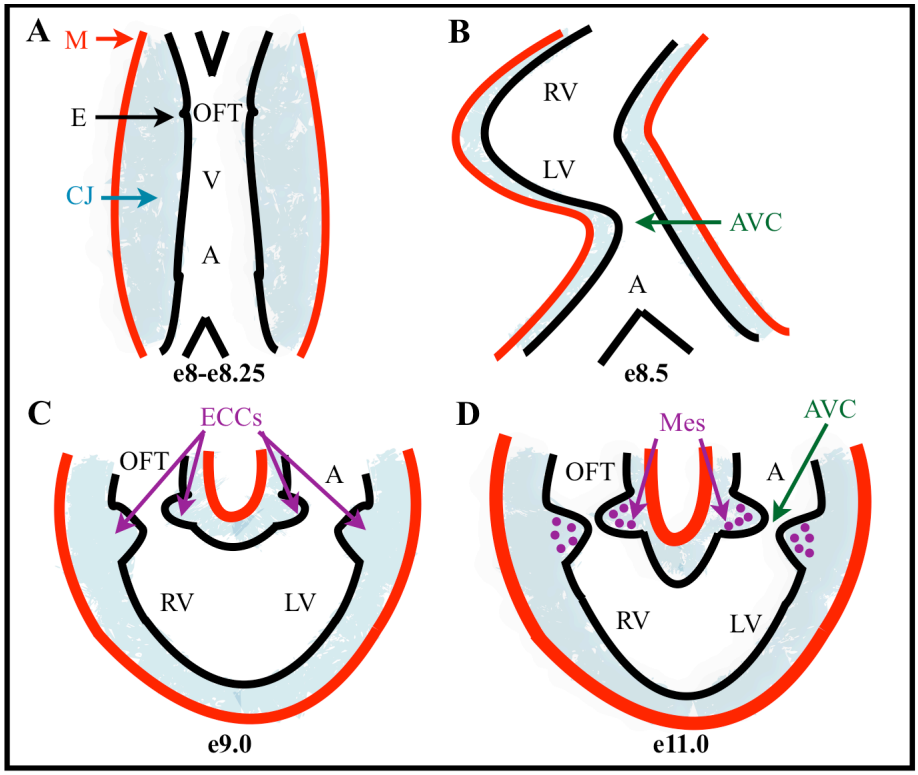

Fig. 1. Overview of early heart development. **A:** At mouse embryonic day (e) 8.0-e8.25, the heart is a tubular structure consisting of an outer myocardial layer (M) and an inner endocardial layer (E) separated by region of extracellular matrix called cardiac jelly (CJ). The linear heart tube is divided into an outflow tract (OFT), a primitive ventricle (V), and a primitive atrium (A). **B:** At e 8.5, the heart begins to loop to the right creating individual chambers including a left ventricle (LV) and right ventricle (RV) as well as the atrioventricular canal (AVC). **C:** Outpouchings of cardiac jelly called endocardial cushions (ECCs) form between the atrium and ventricle and in the OFT. **D:** As the ECCs grow, they become populated with mesenchymal cells (Mes).

cells, and migrate into the cardiac jelly clearly demonstrating that the mesenchymal cells originated from this cell layer (7). This process, called epithelial to mesenchymal transformation (EMT), has been implicated at other time points during embryogenesis including gastrulation and neural crest development (3), as well as in adult organisms during tissue regeneration, organ fibrosis and cancer progression (8).

EMT at the area of the ECCs is a multistep process. An *in vitro* model of EMT was created by explanting AV canal isolates onto collagen gels (Fig. 2A). Studies using this model demonstrated that the myocardium of the AV canals secretes soluble

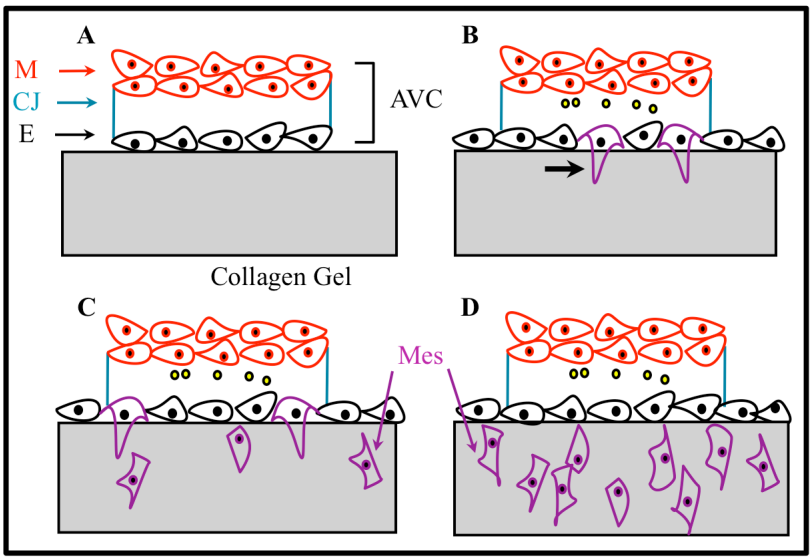

Fig. 2. Overview of the epithelial to mesenchymal transformation (EMT) *in vitro*. **A:** A section of the atrioventricular canal (AVC) containing myocardium (M), cardiac jelly (CJ), and endocardium (E) is explanted onto collagen gel. **B:** The myocardium secretes soluble signaling molecules which induce the underlying endocardium to become activated. Activated endocardial cells extend filapodia (arrow) into the collagen gel. **C:** The new mesenchymal cells (Mes) migrate away from the endocardial layer. **D:** EMT progresses and endocardial cell proliferation continues to maintain a continuous cell layer.

signaling molecules to induce the overlying endocardium to initiate EMT (Fig. 2B). The endocardium of the AV canals is uniquely able to respond to these signals as endocardium isolated from other cardiac regions such as the ventricles is not capable of undergoing EMT (9-11). After AV canal endocardial cells receive the myocardial stimulus, their rough endoplasmic reticula and Golgi complexes hypertrophy thus developing an increased secretory potential. Scanning electron microscopy reveals cell separation corroborating molecular studies which demonstrate a down-regulation of cell-cell adhesion molecules. The activated endocardial cells extend filapodia into the cardiac jelly, and between e9.5 and e10.0 the new mesenchymal cells migrate away from the endocardial cell layer (Fig. 2C). During this process, endocardial cell proliferation continues, possibly to maintain a contiguous endocardial layer (Fig. 2D). After the ECCs

are populated by mesenchymal cells, a series of differentiation events occurs including fusion of the inferior and superior AV cushions to form the AV septum and remodeling of the valves into thin leaflets (3).

1c. EMT is a Carefully Regulated Process with Multiple Signaling Cascades

EMT in the ECCs has been shown to be dependent on a number of signaling pathways including Wnt, Notch, TGF-β, NFATc1, ErbB2/3, EGFR, BMP, and NF1 (Fig. 3). Individual mutations in any of these pathways leads to a defect in EMT suggesting that each pathway is necessary for ECC development (2,3). While some of the downstream signaling molecules in each of these pathways have been identified as being important for EMT, the interactions between the pathways is less well known. The EMT inductive stimulus is comprised of members of the transforming growth factor-β (TGF-β) superfamily, which includes TGF-βs and bone morphogenic proteins (BMPs). The myocardium overlying the ECC endocardium secretes these cytokines (3). *In vitro* studies demonstrate that TGF-β1 or TGF-β2 cultured with ventricular myocardium can induce EMT in explanted AV canal endocardium suggesting that TGF-βs are the inductive agents secreted by AV myocardium *in vivo* (12). BMP-2 has been shown to increase TGF-β2 expression in AV canal explants and can induce EMT in the absence of AV canal myocardium (13). The TGF-β superfamily utilizes intracellular signaling mediators including the Smad proteins, which form heterodimers capable of translocating to the nucleus to activate gene transcription. Downstream TGF-β2 signaling is mediated in part by Slug, a transcription factor required for EMT at other sites in vertebrate development (14). The Snail/Slug family promotes migratory phenotypes by interfering

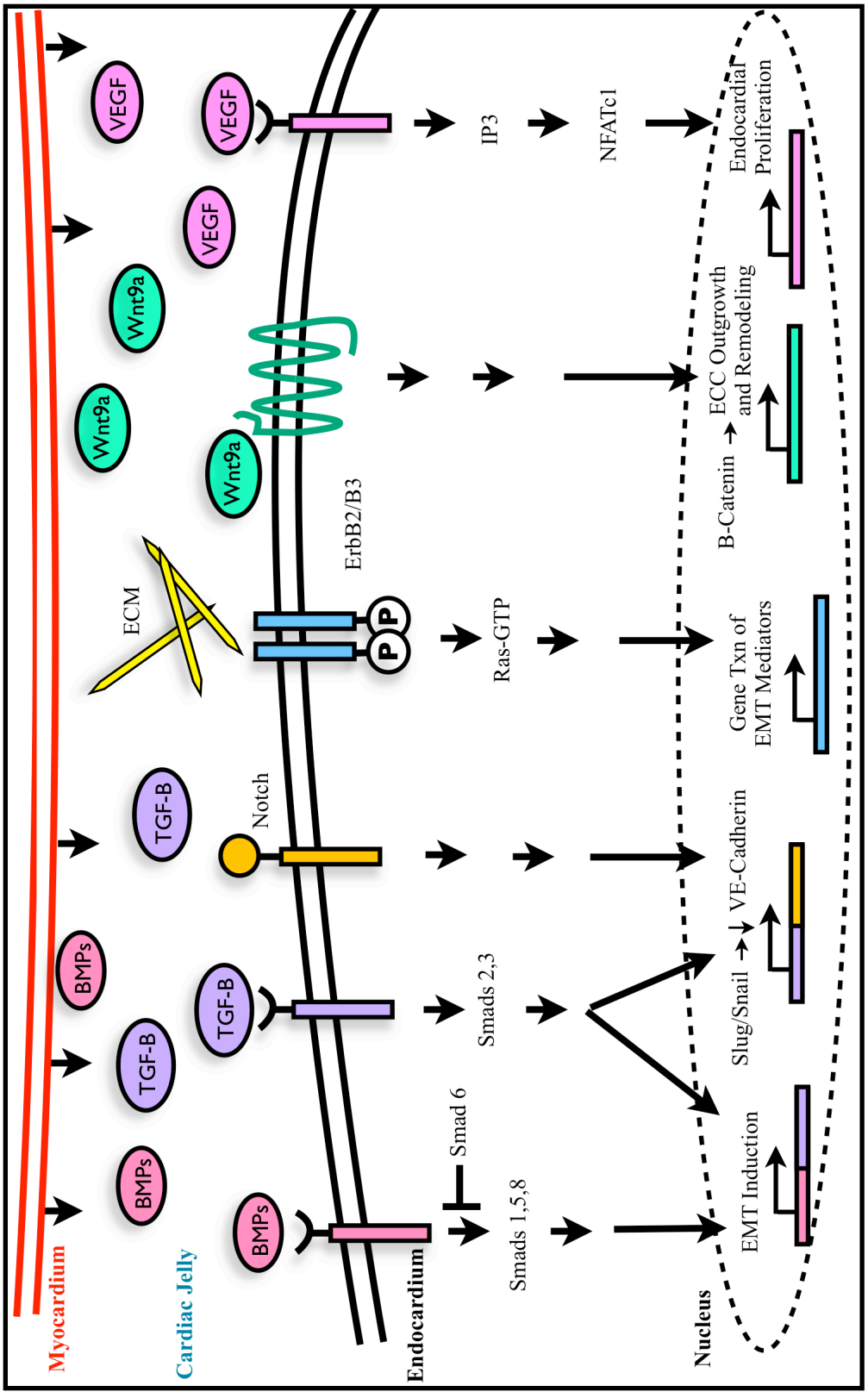

Fig. 3. Signaling pathways involved in EMT. Numerous pathways, including BMP, TGF-B, Notch, ErbB, Wnt9a, and VEGF, must all function together for EMT to occur in the ECCs.

with E-cadherin-mediated cell-cell attachments (3). Another EMT signaling molecule, Notch, is also thought to function via the Slug pathway (2). An additional pathway, the ErbB2/B3 pathway, which will be discussed in detail later, interacts with components of the ECM and signals through Ras to promote EMT (15).

Vascular endothelial growth factor (VEGF), expressed in the AV myocardium, has been implicated in endocardial cell proliferation within the ECCs. Tight control of VEGF levels during development is necessary for proper ECC formation, as mice with both an over-expression and under-expression of VEGF have hypoplastic ECCs (16-18). VEGF signals through IP_3 and NFATc1 (2). Wnt9a, a growth factor that directs differentiation, proliferation, specification, and migration of different cell types during embryogenesis, is expressed in the ECCs and has been shown to be necessary for cell proliferation. Wnt9a signals through B-catenin to promote cardiac cushion outgrowth and remodeling (3). Together, these signaling pathways function to promote EMT only in the AV canal and OFT.

2. A Gata4-Erb-Ras-Erk Pathway Promotes EMT

2a. ErbB Receptor Tyrosine Kinases Function in EMT

ErbB receptors play a role in EMT and interact with Gata4, a transcription factor required for heart development (Fig. 4). ErbB3, one of a family of four tyrosine kinase transmembrane receptors (RTKs), has an expression pattern restricted to the endocardium and transformed mesenchyme of the ECCs (19). Mice with an inactivation of ErbB3 have reduced mesenchymal cells in the AV and OFT ECCs leading to hypoplastic valves, congestive heart failure, and death by e13.5. ErbB3 functions by heterodimerizing with

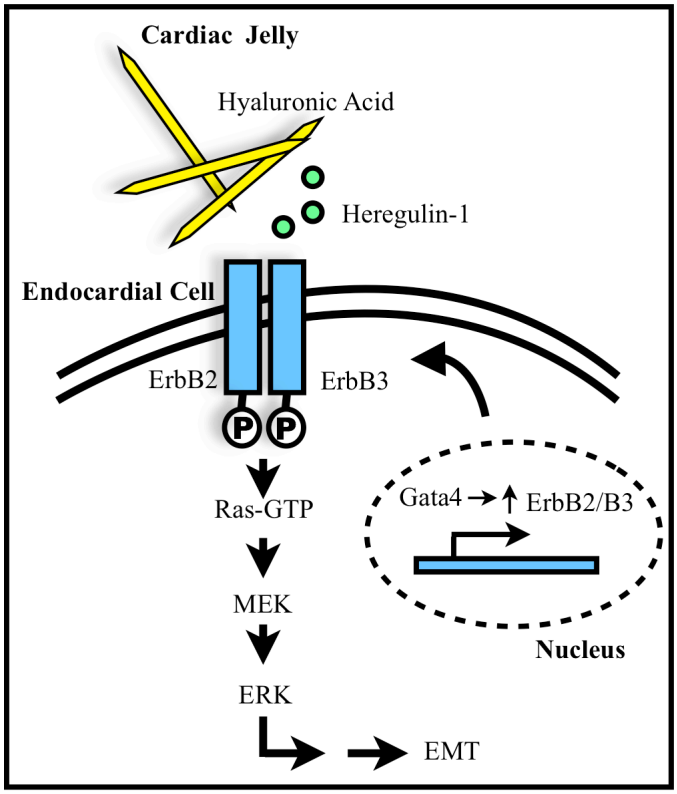

Fig. 4. The Gata4-Erb-Ras-Erk-pathway. Interactions with the ECM component Hyaluronic Acid and the Erb ligand Heregulin-1 are necessary ErbB2 and ErbB3 heterodimerization and activation. Downstream signaling molecules including Ras, MEK, and ERK propagate the signal leading to EMT. The transcription factor Gata4 increases the transcription of ErbB2 and ErbB3. A defect in any component of this pathway leads to defective EMT and hypocellular ECCs.

ErbB2, another RTK, which when knocked out also causes underdeveloped ECCs. This suggests that ErbB2 and ErbB3 function together to promote EMT (19). The factors governing the activation of the ErbB2/ErbB3 heterodimers are complex and involve the ErbB ligand heregulin-1, the cardiac jelly component hyaluronic acid (HA), and the transcription factor Gata4. Defects in any of these components leads to a phenotype resembling that of ErbB3$^{-/-}$ mice, which includes defective EMT in the ECCs (15,19,20).

2b. Hyaluronic Acid and Heregulin-1 are Necessary for Erb Pathway Activation

Embryos with a null mutation in Hyaluronan synthase-2 (Has2) have severe cardiac and vascular abnormalities. Has2 is the source of the glycosaminoglycan hyaluronic acid (HA), which is required for the formation of the cardiac jelly (15). In addition, Has2$^{-/-}$ AV cushion explants lack the ErBB2/ErbB3 phosphorylation necessary

for heterodimerization and activation (21). These phenotypes are rescued by the addition of either HA or the ErbB ligand heregulin-1 (neurogulin-1) (21). Heregulin-1 is normally expressed in the AV canal endocardial cells adjacent to the ErbB3 expressing mesenchymal cells (22). Together, these studies suggest the requirement of HA and heregulin-1 for activation of the ErbB2/ErbB3 pathway.

2c. Gata4 Functions as an Upstream Regulator of the Erb Pathway

Gata4, a zinc finger transcription factor, functions in cell growth and differentiation throughout embryogenesis. Gata4 is first expressed in the embryonic heart at e7.0-7.5 and is localized to the myocardium, endocardium, and ECCs by e9.0 (23,24). This expression pattern and experiments showing that Gata4 is a downstream target of BMPs have led to the suggestion that it may be involved in ECC development (23,25). Although in humans Gata4 heterozygous mutations have been associated with AV septal defects (26), studies using mouse models are difficult as mice with Gata4 deletions fail to develop a linear heart tube and die at e9.0, prior to valve development (23). $Gata4^{T2del}$ mice, which have an endothelial-restricted inactivation of Gata4, survive later in embryogenesis. These mice have hypocellular ECCs, a thinned cushion endocardial cell layer (Fig.5), and variable expression of a thinned myocardium, phenotypes which are not rescued by addition of HA, heregulin-1, TGF-β, or BMP2. Although $Gata4^{T2del}$ mice do not have an altered gene expression of Notch or Snail, they do have a down-regulation of ErbB3 transcription. This suggests that Gata4 functions as an upstream regulator of the ErbB3 pathway (20).

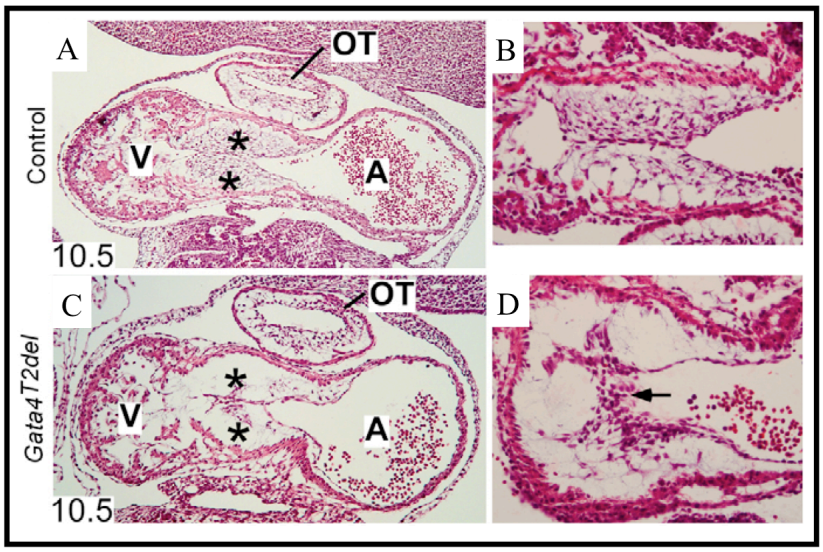

Fig. 5. "Phenotype of embryos with endothelial-restricted inactivation of Gata4 (Gata4T2del). (A-D) Formation of AV cushion mesenchyme requires Gata4 activity in endothelial-derived cells. By E10.5, the AV cushions of control embryos were populated by numerous mesenchymal cells (asterisk, A), whereas in Gata4T2del embryos the AV cushions were severely hypocellular (asterisk, C). The endocardium overlying the AV cushions became several cell layers thick in mutant embryos (arrow, B), whereas it was one cell layer thick in control embryos (D)"(19).

2d. The Signaling Molecules Ras and Erk are Downstream of the Erb Pathway

Continued experiments have shed light on the other signaling molecules necessary for EMT. The role of Ras, a GTPase involved in signal transduction, was first demonstrated in AV cushion explants with experiments showing that infection with adenovirus encoding constitutively active Ras leads to increased EMT and hypercellular ECCs (15, 27). Conversely, infection with dominant negative Ras leads to impaired ECC development. Overexpression of active Ras also rescues the $Has2^{-/-}$ phenotype suggesting that Ras functions downstream of ErbB3 (15). Erk, a member of the MAP kinase family involved in cell proliferation and differentiation, functions downstream of Ras. During ECC development, active Erk is phosphorylated; this phosphorylation is

reduced in Gata4^{T2del} mice suggesting that Gata4 and Erk function in the same pathway (20).

Together, these data support a model for ECC development in which Gata4 functions as an upstream regulator of the ErbB pathway. This pathway requires HA and heregulin-1 for initiation and potentates a signal which converges on Ras and Erk activation.

3. Cilia May Play a Sensory Role in Heart Development

3a. Proper Cardiogenesis Depends on Fluid Flow

Given that the heart is a fluid filled organ which functions to pump blood, it is no surprise that fluid flow is important in early cardiogenesis. This is demonstrated by the chicken venous clip model: after the ligation of one of the vitelline veins, there are immediate changes in blood flow patterns in the heart (28). These chickens eventually develop cardiovascular malformations including ventricular septal defects and semilunar valve anomalies (29). A mouse model has been created with no intracardiac fluid flow secondary to a mutation in an ion transport protein necessary for contraction. The ECCs in these mice do not become seeded with mesenchymal cells. These results support a role for fluid flow in cardiogenesis and in EMT (30).

Endothelial cells have been demonstrated to respond to shear stress, the frictional force of blood along the vessel wall, by regulating expression of shear responsive genes. Both positive and negative shear stress responsive promoter elements (SSRE) and transcription factors have been identified (31). This suggests that endocardial cells may have a way of sensing the changes in fluid flow.

3b. Cilia could be the Link Between Fluid Flow and Downstream Signaling Pathways

Primary cilia, which are located on almost every nondividing cell, have been shown to function as sensors of fluid shear stress in cultured adult kidney epithelial cells (32) and the mouse embryonic node (33), although their role in cardiogenesis has not yet been characterized. Cilia were first described by Zimmerman in 1898 and are found in many tissues across diverse phyla (34). They are composed of a microtubule (MT) core called an "axoneme" consisting of nine peripheral MT doublets, with ("9+2") or without ("9+0") a central pair of MTs. Although some overlap in function exists, 9+2 cilia or motile cilia are found on the apical surfaces of epithelial cells lining such surfaces as the airway and oviduct, while the 9+0 cilia are immotile and protrude from the cell membranes of most cell types (35,36).

The first evidence of cilia on cardiovascular endothelial cells was from cultured bovine aortic cells (37) and 22-24 week human fetal aortas (38). In the chicken embryonic heart, cilia are present at Hamburger and Hamilton (HH) stages 24-30 (corresponding to mouse e12.5-14), a time characterized by valve remodeling and AV septum formation. Cilia are observed at greater concentrations on endocardial cells located in areas of low shear force (39). The inverse relationship between cilia concentration and shear stress is supported by studies using human umbilical vein endothelial cells (HUVEC), which demonstrate that cilia disassemble when exposed to high laminar shear stress. This disassembly is thought to be secondary to the termination

of intraflagellar transport (IFT), the process necessary for ciliary biogenesis and protein shuttling (40).

Cilia are involved in activating shear stress responsive genes in chicken heart endothelial cells (CHEC). When ciliated and non-ciliated CHEC cells are exposed to fluid flow, ciliated CHEC have an increased induction of a shear-responsive transcription factors (41). The relationship between cilia and fluid flow is not unexpected as cilia function as mechanosensors and chemosensors at other times during development. Mutations in cilia proteins, termed "ciliopathies," underlie a variety of human disorders including situs inversus, polycystic kidney disease, retinal degeneration, pancreatic and liver cysts, hyodrocephaly, and skeletal abnormalities (34,42).

3c. Cilia are Multifunctional Organelles involved in Left-Right Development

The first link between cilia and cardiogenesis came from human studies which suggested that cilia are mediators of the development of left-right (LR) asymmetry (33). Primary ciliary dyskinesia (PCD) is a recessive genetic disorder caused by mutations in genes that encode for ciliary motility. These patients have randomization of LR development: about half of patients will have a normal orientation of the heart and viscera (*situs solitus*), while the other half, also known as Kartagner's Syndrome, will have a mirror image reversal (*situs inversus*). PCD patients also have respiratory compromise and male infertility due to the inability of cilia to perform their normal functions in the trachea and on sperm (43). Further studies on animal mouse models have demonstrated two types of cilia located on the embryonic node, the location of the signaling cascade responsible for the development of LR asymmetry. Motile cilia

contain the axenomal left-right dynein (lrd) which enables coordinated beating of the cilia to generate leftward nodal flow (44), while immotile cilia function as sensory cilia. These sensory cilia express the cation channel polycystin-2 (pkd-2), and respond to the nodal flow by generating an increase in intracellular calcium at the left side of the node (33).

3d. Cilia Mutant Mice have Numerous Cardiovascular Defects

While studying the role of cilia in LR development, numerous mutations affecting ciliary biogenesis, motility, or sensory function have been identified and characterized (Table 1) (33,45-48). In addition to defects in LR development, many of these mice have complex cardiac defects. Although some degree of cardiac malformation can be explained by the incorrect cardiac looping along the LR axis, the differences observed between the different cilia mutants suggest a larger role for cilia in cardiogenesis. 40% of mice and 6.5% of humans with mutations leading to immotile but structurally normal cilia have intracardiac defects (49-51). Conversely, 100% of mice with defects in ciliary biogenesis or mechanosensation have intracardiac defects. Mice with mutations in the kinesin-II motor complex proteins, Kif3a and Kif3b, which have a complete absence of cilia, develop heart failure and die at e10.9-12.5 independent of LR axis development (46,52). In addition, mutations in the mechanosensory protein, pkd-2, lead to a 100% penetrance of cardiac defects such as AV canal defects (47). These defects occur regardless of *situs,* as up to half of these mice will actually have normally looped hearts positioned properly along the LR axis. These findings suggest that cilia have a function in cardiogenesis beyond that of LR determination.

Table 1. Known Ciliary Mutations Included in our Experiments.

Mutation	Ciliary Defect	Lethality	Cardiac Phenotype
Lrd (Left-right dynein	Motility	40% long term survival	40% normal, some AV canal and other CHD
Inv (Inversin)	Unknown, but present	~100% at post-natal day 5	100% situs inversus, some with CHD
Kif3a (Kinesin)	Ciliary Biogenesis	E10.5	100% pericardial effusion, myocardial thinning, congestive heart failure
Ift (Intraflagellar Transport)			
Pkd (Polycystic kidney disease)	Mechanosensation	E14.5-16.5	Pericardial effusion, AV canal defects

To further investigate the role cilia have in heart development, we first performed immunohistochemistry to demonstrate that cilia are present in the mouse heart at e9.5 and e12.5. In addition, we characterized the heart defects in three cilia mutant mice further demonstrating the importance of cilia in cardiogenesis, specifically EMT and the formation of the compact myocardium (CM). We also looked at Gata4 expression in four cilia mutant mice and suggest that cilia and Gata4 function in interacting pathways to promote ECC development.

Statement of Purpose and Specific Aims

Hypothesis: Given the role that cilia play in the development of other fluid filled organs, we expect cilia to be important in cardiac morphogenesis independent of their role in left-right development.

Aim 1: Using immunohistochemistry to stain for cilia in wild-type embryos, we will determine the timing and location of cardiac cilia.

Aim 2: By comparing sectioned hearts of mice with mutations affecting ciliary biogenesis, motility, and mechanosensation, we will analyze the structural abnormalities and thus characterize the specific role cilia play in cardiogenesis.

Aim 3: Using *in situ* hybridization with Gata4, a transcription factor involved in heart development, we will compare the Gata4 expression pattern in ciliary mutants to determine what, if any, interaction cilia have with Gata4.

Methods

Mice[1]

Lrd$^{\Delta neo/\Delta neo}$ mice were previously generated in this lab by placing an in-frame fusion of GFP into the N-terminal of lrd, and placing the neomycin resistance gene flanked by loxP sites into the first intron of lrd. The resulting lrd$^{\Delta neo/\Delta neo}$ mice have a high incidence of *situs inversus* and perinatal lethality and due to a splice abnormality fail to make any full-length lrd message (33). Kif3a$^{fl/fl}$ mice were obtained from Larry Goldstein (University of California, San Diego) (46), and Kif3a$^{-/-}$ mice were obtained by crossing Kif3a$^{fl/fl}$ mice with mice expressing Cre recombinase under the control of the actin promoter. Pkd2$^{+/-}$ mice were obtained from Stefan Somlo (Yale University School of Medicine) (53). IFT$^{+/-}$ mice were obtained from Greg Pazour (University of Massachusetts Medical School) (45). Inv$^{+/-}$ mice were obtained from Paul Overbeek (Baylor College of Medicine) (48).

Embryos were obtained from timed intercrossing of heterozygous mice for Kif3a$^{-/-}$, Pkd2$^{-/-}$, Inv$^{-/-}$, and IFT$^{-/-}$ mice and from homozygous crosses for lrd$^{\Delta neo/\Delta neo}$ mice. Noon of the day of detection of the vaginal plug was considered as 0.5 dpc.

Embryo Dissection, Preparation, and Genotyping[2]

To obtain embryos for the experiments, the mother was sacrificed either 8.5, 9.5 or 12.5 days after conception. The embryos were dissected in PBS and a section of

---

[1] Mice were generated or obtained by Martina Brueckner or Svetlana Makova and mice crosses were performed by Jeffery Drozd.

[2] I performed all dissection and genotyping of e9.5 Kif3a$^{-/-}$, Pkd2$^{-/-}$, Inv$^{-/-}$, IFT$^{-/-}$ and lrd$^{\Delta neo/\Delta neo}$ embryos used in Gata4 experiments. Embryos used in H&E staining or immunohistochemistry were dissected and genotyped by lab members: Martina Brueckner, Jennifer Slough, Svetlana Makova or Jeffrey Drozd or by me.

membrane was retained for PCR. Embryos were fixed overnight at 4ºC in 4% paraformaldehyde in PBT. Embryos were then dehydrated in graded solutions of methanol and water and stored at 4ºC in 100% methanol. The section of membrane for each embryo was boiled in proteinase K. The following primers were used:

	Forward Primer	Reverse Primer	Third Primer (if used)	Annealing Temp.
$Pkd2^{-/-}$	5'-gcgccggcctagctgtccc-3'	5'-gtgctacttccatttgtcacgtcctgc-3'	5'-gttgtcgcggctccacg-3'	65°C
$Inv^{-/-}$	5'-gacaagtcttacccctgcca-3'	5'-tagcctgacaaagggatggg-3'		58°C
$IFT^{-/-}$	5'-actcagtatgcagcccaggt-3'	5'-gctagatgctgggcgtaaag-3'	5-'ggagcccaggttcagttatgc-3'	55°C
$Kif3a^{-/-}$	5'-agggcagacggaagggtgg-3'	5'-tctgtgagttttgaccagcc-3'	5'-ggtgggagctgcaagaggg-3'	60°C

The PCR products were then run on a 2% agarose gel for genotyping.

Embryo Sectioning using Parafilm[3]

Embryos stored in methanol were rehydrated into PBS and then dehydrated into ethanol. Using graded solutions of water and xylene and then solutions of xylene and wax, embryos were cleared and transferred to parafilm wax. Embryos were mounted in a plastic mold and positioned head down to produce transverse sections. Embryos were sectioned using an American Optical 820 Rotary Microtome into 15µm sections and placed onto slides (about 10 embryos/slide).

Immunohistochemistry[4]

After parafilm embedding and sectioning, the slides were cleared, rehydrated in a series of graded solutions of ethanol and water, and washed in PBS. Antigen retrieval

[3] I performed parafilm embedding and sectioning of e9.5 WT embryos. E9.5 $Kif3a^{-/-}$, $Pkd^{-/-}$ and $lrd^{\Delta neo/\Delta neo}$ embryos were processed by me and Jennifer Slough. E12.5 WT embryos were processed by Jennifer Slough.

[4] I performed immunohistochemistry of e9.5 WT embryos and Jennifer Slough performed immunohistochemistry of e12.5 embryos. I performed all imaging of e9.5 and e12.5 embryos.

was performed using Signet Retrieve All 2 1x. Blocking was performed using 5% goat serum in PBS for 1 hour. Slides were then incubated for 2 hours at room temperature (RT) with mouse monoclonal anti-acetylated tubulin clone 6-IIB-1 (Sigma) at a 1:200 dilution in 5% goat serum. Four 20-minute washes were performed in PBS-0.1% Tween 20 (PBT; American Bioanalytica) at RT. Slides were then incubated for 45 minutes at RT in a 1:200 dilution of Texas Red-conjugated anti-mouse antibody in 5% goat serum followed by four 20-minute washes in PBT at RT. A 1:1,000 dilution of Hoeschst (Molecular Probes) was added to wash three. The slides were rinsed in water and cover-slipped using ProLong Antifade reagent with DAPI (Invitrogen). Sections were examined with a Zeiss Axiovert microscope equipped with Apotome imaging.

H&E staining[5]

Cleared and rehydrated slides were stained in Mayer's Hematoxylin Solution for one minute, rinsed, and placed in Reagent Alcohol 95% for 30 seconds. The slides were then placed in Eosin Y Solution Counterstain for one minute, dehydrated, cleared, and mounted with resinous mounting medium. Sections were examined with a Zeiss Axioskop microscope.

Whole Mount *In-Situ* Hybridization (WMISH)[6]

Steps were performed as previously described (54) and are detailed below.

Preparation of Gata4 probe

[5] I performed H&E staining and imaging of all e9.5 and e12.5 WT embryos.
[6] I prepared the Gata4 probe and performed all *in situ* hybridizations of Kif3a$^{-/-}$, Pkd2$^{-/-}$, Inv$^{-/-}$, IFT$^{-/-}$ and lrd$^{\Delta neo/\Delta neo}$ embryos.

Following bacterial transformation and DNA extraction, Gata4 DNA was linearized by digestion with restriction enzyme ecoRV (New Endgland BioLabs) at 37 ºC for 2 ½ hours. The size of the band was confirmed by running 5µl of digest on a 1% agarose gel. The linearized DNA was incubated for 30 minutes at 37ºC with 200ug/ml proteinase K and 0.5% SDS. A phenol/chloroform extraction and ethanol precipitation were performed and the pellet was resuspended in 20µl of TE. DNA concentration was determined by running 1µl of DNA on a 1% agarose gel and comparing it to the DNA ladder.

A labeling reaction was set up as follows:

Gata 4 DNA	4µl
Buffer	2µl
DIG	3µl
25mM MgCl	3.2µl
RNAi	0.5µl
SP6 (RNA polymerase)	2µl
Deionized water	5.3µl

This probe reaction was incubated at 37ºC for two hours, an additional 2µl of SP6 polymerase was added, and the reaction was incubated for another hour. A LiCl/ethanol precipitation was performed and the solution was incubated overnight at -20ºC. The solution was centrifuged and the pellet was washed in 80% ethanol. The labeled RNA was dissolved in 25 μl Rnase-free water. The probe was confirmed on 1% agarose gel.

WMISH Day 1 Probe Hybridization

Embryos are removed from storage in methanol and rehydrated in graded solutions of methanol and PBT. Embryos were incubated at RT in 10µg/ml proteinase K in PBT for 10 minutes, rinsed in PBT, incubated for 30 minutes in PGF post-fixation solution,[7] and rinsed in PBT. Embryos were incubated in graded solutions of PBT and

[7] Paraformaldehyde/glutaraldehyde fixative (PGF): 4% paraformaldehyde, 0.025% glutaraldehyde in PBS

hybridization (hyb) buffer.[8] Embryos were then incubated at 70ºC in 2.4 ml of hyb buffer. After 1 hour, 2.4 μl of Gata4 probe was added and the embryos were incubated overnight.

WMISH Day 2 Antibody Reaction

Embryos were incubated in the following solutions at 70ºC: two rinses in hyb buffer, two 30-minute washes in hyb buffer, and a 10 minute wash in a 1:1 solution of hyb buffer and TBST (1X TBS, 0.1% Tween-20). Embryos were incubated in the following solutions at RT: two rinses in TBST, a 15 minute wash in TBST, an hour wash in Blocking Buffer A,[9] and an hour wash in Blocking Buffer B.[10] Embryos were incubated overnight at 4ºC, rocking, in 3ml of Blocking buffer B with 2 μl of Anti-Digoxigenin-AP Fab fragments (Roche Diagnostics).

WMISH Day 3 Detection

Embryos were washed in three 1-hour washes of TBST with gently rocking, rinsed with water, and incubated with BM Purple AP Substrate (Roche Diagnostics) in the dark for 4 hours. Embryos were imaged using a Zeiss Apolumar microscope.

Embryo Sectioning with Frozen Sections[11]

Gata4 embryos were overdeveloped in BM Purple AP Substrate at RT for 5 hours and at 4ºC overnight. Embryos were rinsed three times with PBT and post-fixed (4% paraformaldehyde, 0.1% glutaraldehyde in PBS) at RT for 2 hours. Embryos were washed with PBS and incubated in 20% sucrose in PBS at 4ºC overnight. In the morning, embryos were blotted to remove all of the sucrose solution and transferred to

---

[8] Hybridization buffer: 50% formamide (Boehringer Mannheim), 0.75 *M*NaCl, 1X PE, 100 µg/mL tRNA (Sigma R-5636, 10 mg/mL solution), 0.1% BSA, 1% SDS, 0.1% Tween-20, in DEPC water; made fresh each time; pre-warmed to 70ºC

[9] Blocking Buffer A: TBST with 2% BBR

[10] Blocking Buffer B: TBST with 2% BBR and 20% goat serum

[11] I performed all frozen sectioning and imaging.

Tissue Tek O.C.T. Compound (Sakara Finetek). Embryos were incubated in O.C.T. at 4ºC for 4 hours, transferred to a specimen mold, and positioned with the embryo head down. Molds were filled with O.C.T., flash frozen using a Styrofoam bath filled with ethanol and dry ice, and stored at -80ºC overnight and until sectioning. Embryos were sectioned using Leica CM3050 S Cryostat into 15µm sections and placed onto slides (about 10 embryos/slide). Slides were rinsed with water and counterstained with 200µl of Nuclear Fast Red (1:4 dilution) for one minute before rinsing with water for 5 minutes. When dry, slides were mounted with Cryoseal 60 (Richard Allan Scientific) and imaged using a Zeiss Axioskop microscope.

Results

Cardiac Cilia are Present Throughout the Embryonic Mouse Heart During Different Time Points

In order to investigate the role that cilia play in cardiac morphogenesis, it is necessary to first demonstrate their presence on key heart structures at critical times in cardiac development. We examined mouse hearts at embryonic day (e) 9.5 and e12.5, time points which encompass a common point of lethality for severe ciliary mutants, to characterize the location of cilia before and after important morphological changes. At e9.5, heart looping has occurred, but a common atrial chamber and a common ventricular chamber persist, while by e12.5 the ECCs have commenced to form the AV septum and valves. To identify cilia, we immunolabeled parafilm-embedded embryo sections with antibodies against acetylated tubulin, a protein found in cilia as well as other structures which contain stable microtubules such as mitotic spindle and midbodies.

As shown in Fig. 6, cilia are widely distributed throughout the e9.5 mouse heart. Cilia are present on the atrial endocardial cells and protrude into the atrial lumen (Fig. 6D). A few cilia are seen on the compact ventricular myocardial cells (yellow arrows in Fig. 6E). At e9.5, the ventricles show early signs of trabeculation, and we observe prominent cilia on the endocardial layer surrounding the trabeculations (Fig. 6G). Cilia are located on the luminal surface of early ECC endocardium where they protrude into the atrial cavity (yellow arrows in Fig. 6F). They are also present on the early ECC mesenchymal cells in random orientation (white arrows in Fig. 6F).

Fig. 7 shows the persistence of cilia in the e12.5 heart. This time point is characterized by the progression of atrial and ventricular septation and the appearance of

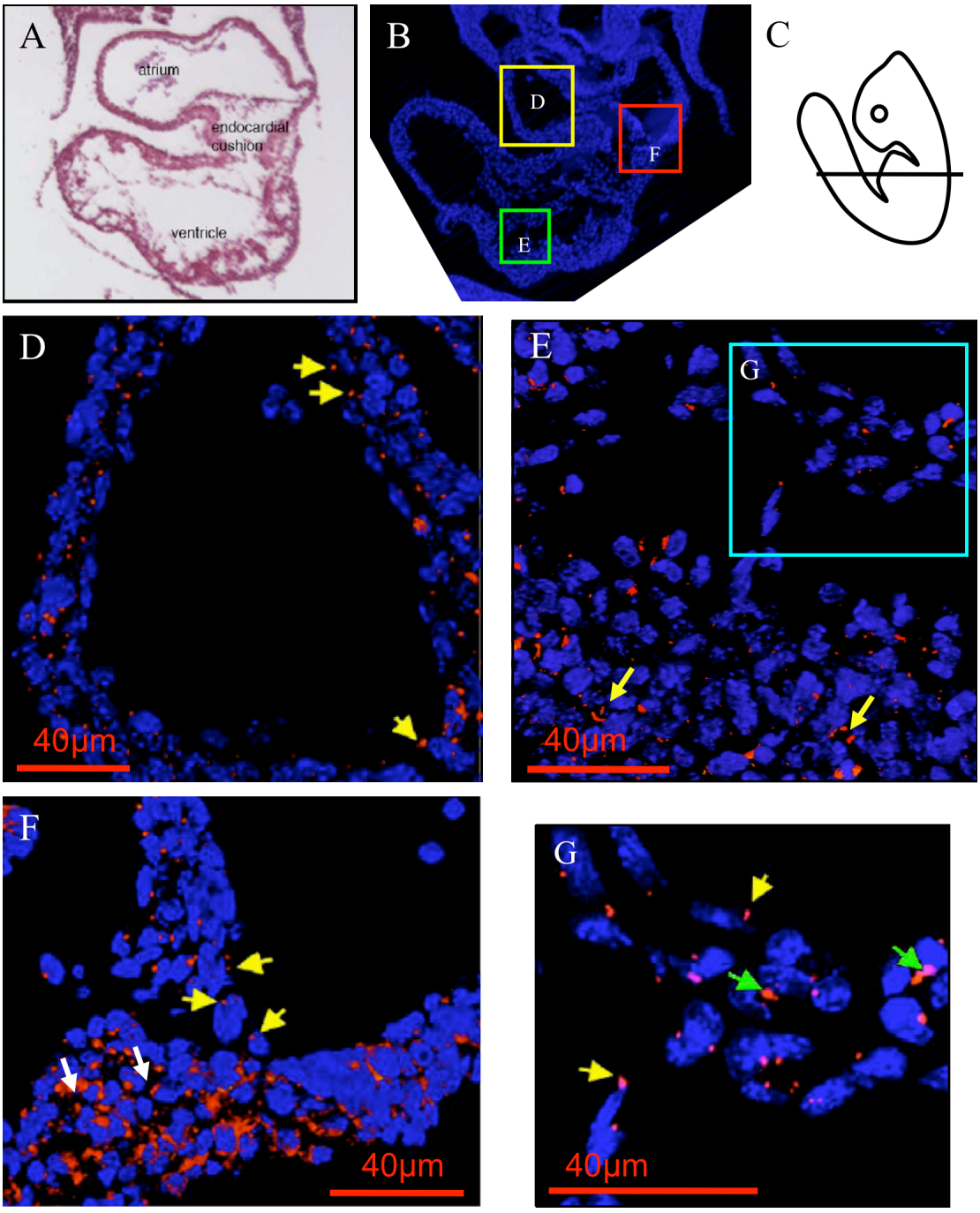

Fig. 6. Distribution of cilia in the e9.5 mouse heart. **A-B:** Cross-section of an e9.5 mouse heart stained with hematoxylin and eosin (**A**) and Hoechst (nuclear) fluorescence (blue) (**B**). Boxed outline panels enlarged in D-F. **C:** Diagram showing level of transverse sections. **D-G:** All images are projection of Z stacks taken through the 15-μm section at a level of 0.35-μm. Anti-acetylated tubulin labels cilia in red (yellow and white arrows) in addition to mitotic spindle and mid-bodies (green arrows). **D:** Atrium. **E:** Ventricular compact myocardium (yellow arrows) and early trabeculations. **F:** Early ECC, showing cilia on both endocardial (yellow arrows) and mesenchymal cells (white arrows). **G:** Magnification of ventricular trabecular myocardium.

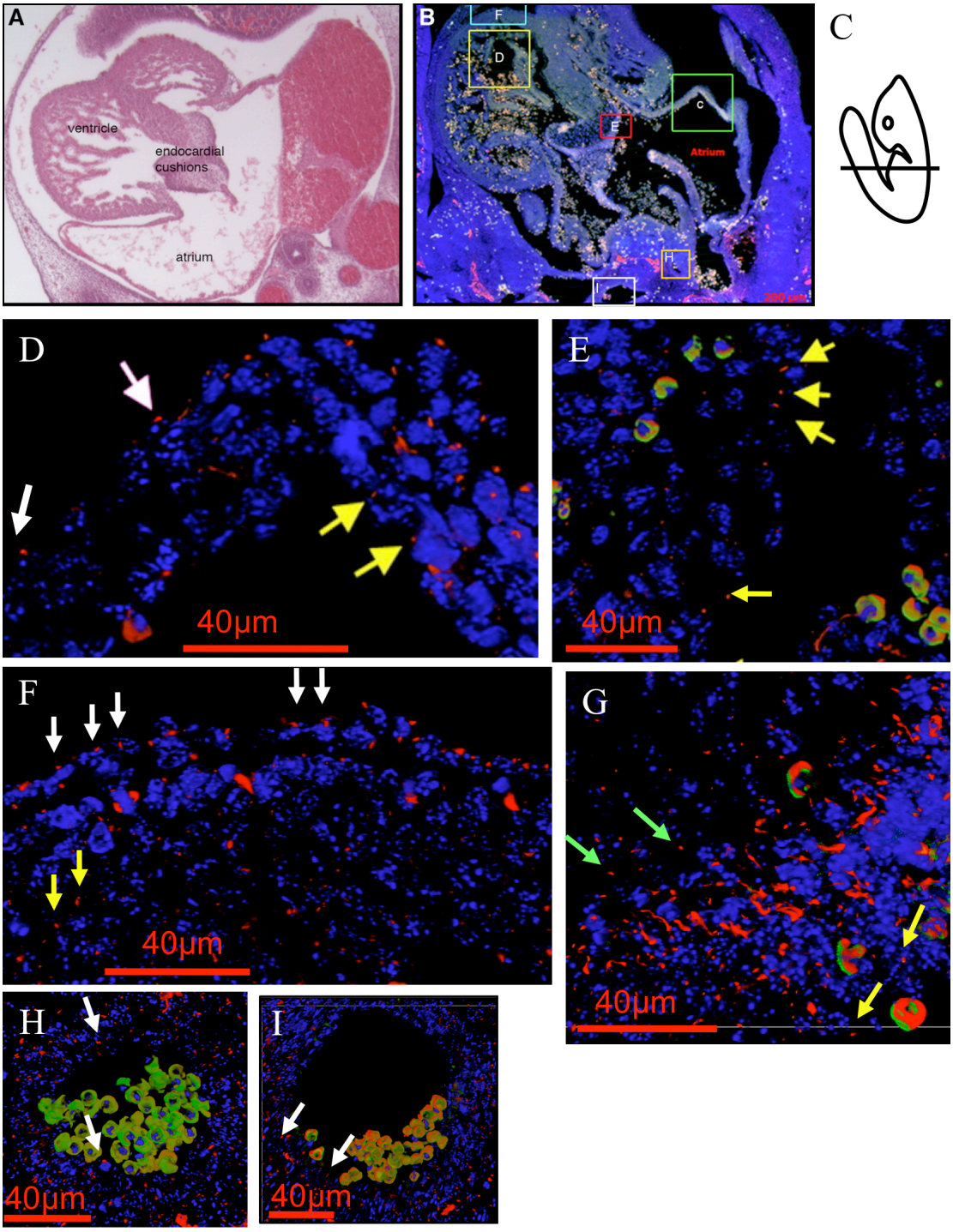

Fig. 7. Distribution of cilia in the e12.5 mouse heart. **A-B:** Cross-section of an e12.5 mouse heart stained with hematoxylin and eosin (**A**) and Hoechst (nuclear) fluorescence (blue) (**B**). Boxed outline panels enlarged in D-I. **C:** Diagram showing level of transverse sections. **D-I:** All images are projection of Z stacks taken through the 15-µm section at a level of 0.35-µm. Anti-acetylated tubulin labels cilia in red. Red blood cells autoflouresce in green and red channels. **D:** Cilia on atrial epicardium (white arrows) and endocardium (yellow arrows). **E.** Ventricular trabeculations. **F:** Cilia on ventricular epicardium (white arrows) and compact myocardium (yellow arrows). **G:** ECC showing cilia on both endocardial surface (yellow arrows) and mesenchymal cells (green arrows). **H:** Artery. **I:** Vein.

a prominent mesenchymal component in the ECCs. Blood can be seen in the atria and ventricles as well as the developing blood vessels (Red blood cells autofluoresce and are visible as combined red and green fluorescence in Fig. 7E). A few cilia continue to be visible on the atrial endocardial cells (yellow arrows in Fig. 7D) but to a lesser degree than at e9.5. A striking difference between the e9.5 and e12.5 hearts is the presence of cilia on the epicardial surface of the atria (white arrows in Fig. 7D) as well as the ventricles (white arrows in Fig. 7F). Cilia on the ventricular epicardium are present at a ratio of one cilium per cell and extend toward the pericardial space (white arrows in Fig. 7F). We observe cilia on the compact ventricular myocardium (yellow arrows in Fig. 7F) as well as the trabecular myocardium where they extend into the ventricular cavity (Fig. 7E). At e12.5, the epithelial to mesenchymal transformation (EMT) occurring in the ECCs has progressed and the ECCs are at the early stages of remodeling to form the atrioventricular (AV) valves and septum. Cilia are widely dispersed on both the endocardial surface (yellow arrows in Fig. 7G) and the forming mesenchymal cells (green arrows in Fig. 7G). A new feature of the e12.5 heart is the presence of developing blood vessels. Many cilia are seen in the walls of the arteries (Fig. 7H) and veins (Fig. 7I) although only a few cilia extend into the vessel lumens.

These data demonstrate the presence of cilia in the atria, ventricles, ECCs, epicardium, and blood vessels in mice hearts during times critical to cardiac development where they could function in developmental pathways. Furthermore, the presence of cilia on the ECCs before and after EMT progression supports a potential role for cilia in EMT.

Mice Without Cilia have Hypocellular Endocardial Cushions and Thinned Compact Myocardium

To further characterize the phenotype of mice with ciliary mutations, we examined the hearts of e9.5 wild-type, $lrd^{\Delta neo/\ \Delta neo}$ (lrd $^{-/-}$, defective ciliary motility), $Pkd2^{-/-}$ (defective ciliary mechanosensation) and $Kif3a^{-/-}$ (defective ciliary biogenesis) embryos. Embryos were fixed and embedded in parafilm and then transverse sections were stained with hematoxylin and eosin (H&E). $lrd^{\Delta neo/\ \Delta neo}$, $Pkd^{-/-}$, and $Kif3a^{-/-}$ mice have been previously shown to have defects in left-right (LR) positioning. As a result, we chose to only analyze D-looped hearts, enabling us to conclude that any heart defects we observed were a direct result of the role cardiac cilia place in heart development and were not due to abnormal heart looping. At e9.5, the endocardial cells in the ECCs are beginning to undergo transformation into mesenchymal calls. We counted the number of mesenchymal cells in three adjacent 15 μm sections from two independent embryos of each genotype: WT – 66 cells/section, $lrd^{\Delta neo/\ \Delta neo}$ – 32 cells/section, $Pkd2^{-/-}$ – 46 cells/section, $Kif3a^{-/-}$ – acellular.

We observed that the $lrd^{\Delta neo/\ \Delta neo}$ embryos were grossly comparable to wild-type (Fig. 8A). They have slightly decreased ECC cellularity (Fig. 8B), however the ventricular trabeculations and epicardium appear normal (Fig. 8C). The compact myocardium (CM), assessed at the ventricular apex, was found to be 2-3 cell layers thick, which is similar to wild type (Fig. 8C). The heart of the $Pkd2^{-/-}$ embryo has a few visible defects including a slight pericardial effusion (Fig. 8A) and decreased cellularity of the ECCs compared to wild-type (Fig. 8B). The trabecular myocardium appears normal, but the CM is thinner than wild-type (Fig. 8C). The $Kif3a^{-/-}$ embryos have the most striking

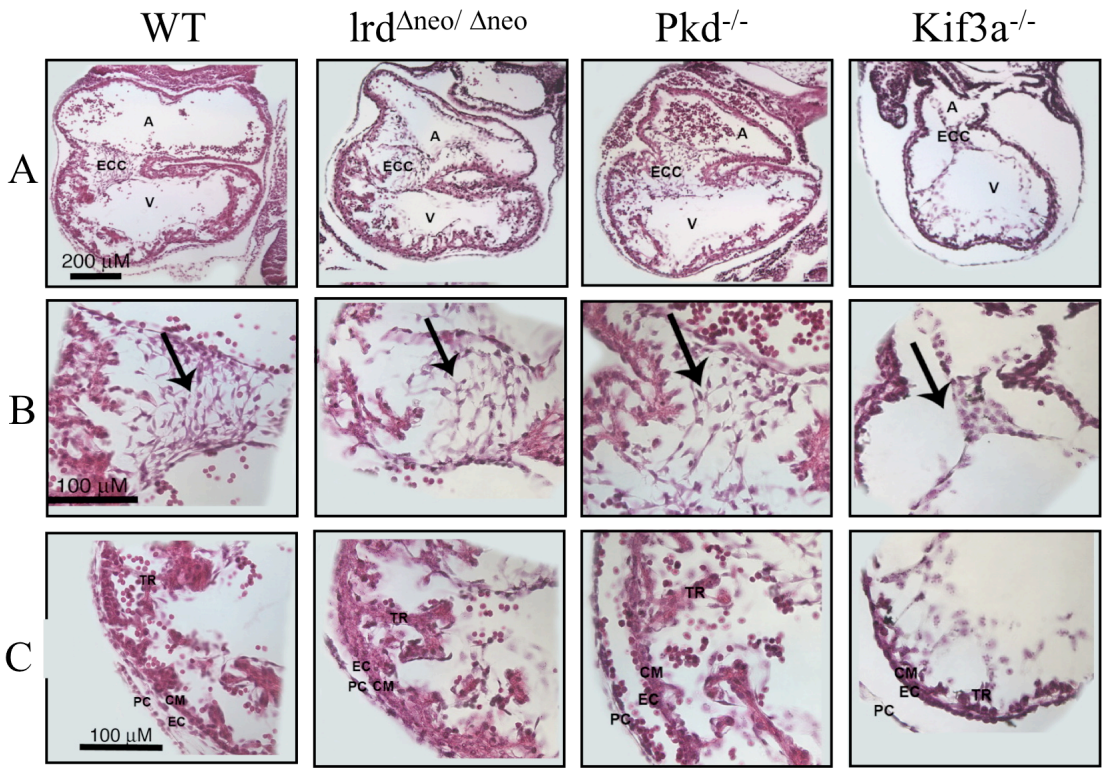

Fig. 8. Cross-sections of e9.5 wild-type, lrd$^{\Delta neo/\ \Delta neo}$, Pkd2$^{-/-}$, and Kif3a$^{-/-}$ mouse hearts stained with hematoxylin and eosin. **A:** Overview of wild-type, lrd$^{\Delta neo/\ \Delta neo}$, Pkd2$^{-/-}$ and Kif3a$^{-/-}$ hearts showing the atrium (A), ventricle (V), and endocardial cushions (ECC) at the region of the inflow tract. **B:** Magnified view of the ECCs, showing decreased cushion cellularity in the Kif3a$^{-/-}$ embryo. Arrow indicates mesenchymal cells. **C:** Magnified view of ventricular trabeculations (TR), compact myocardium (CM), epicardium (EC), and pericardium (PC) showing decreased trabeculations in the Pkd2$^{-/-}$ section and no trabeculations in the Kif3a$^{-/-}$ section.

phenotype. A large pericardial effusion surrounds the heart (Fig. 8A). The ECCs are almost completely acellular, consisting only of endocardial cells and no mesenchymal cells (arrow in Fig. 8B). The ventricles in the Kif3a$^{-/-}$ embryos have significantly decreased trabeculations and the CM is only a single cell layer thick (Fig. 8C).

Higher magnification of the compact and trabecular myocardium reveals normal structures in wild-type and lrd$^{\Delta neo/\ \Delta neo}$ embryos (Fig. 9B). Although Pkd2$^{-/-}$ embryos have a normal pericardium, epicardum and trabecular myocardium, the CM is thinned, reaching one cell layer in some locations (Fig. 9B). In the Kif3a$^{-/-}$ embryo (Fig. 9B), a

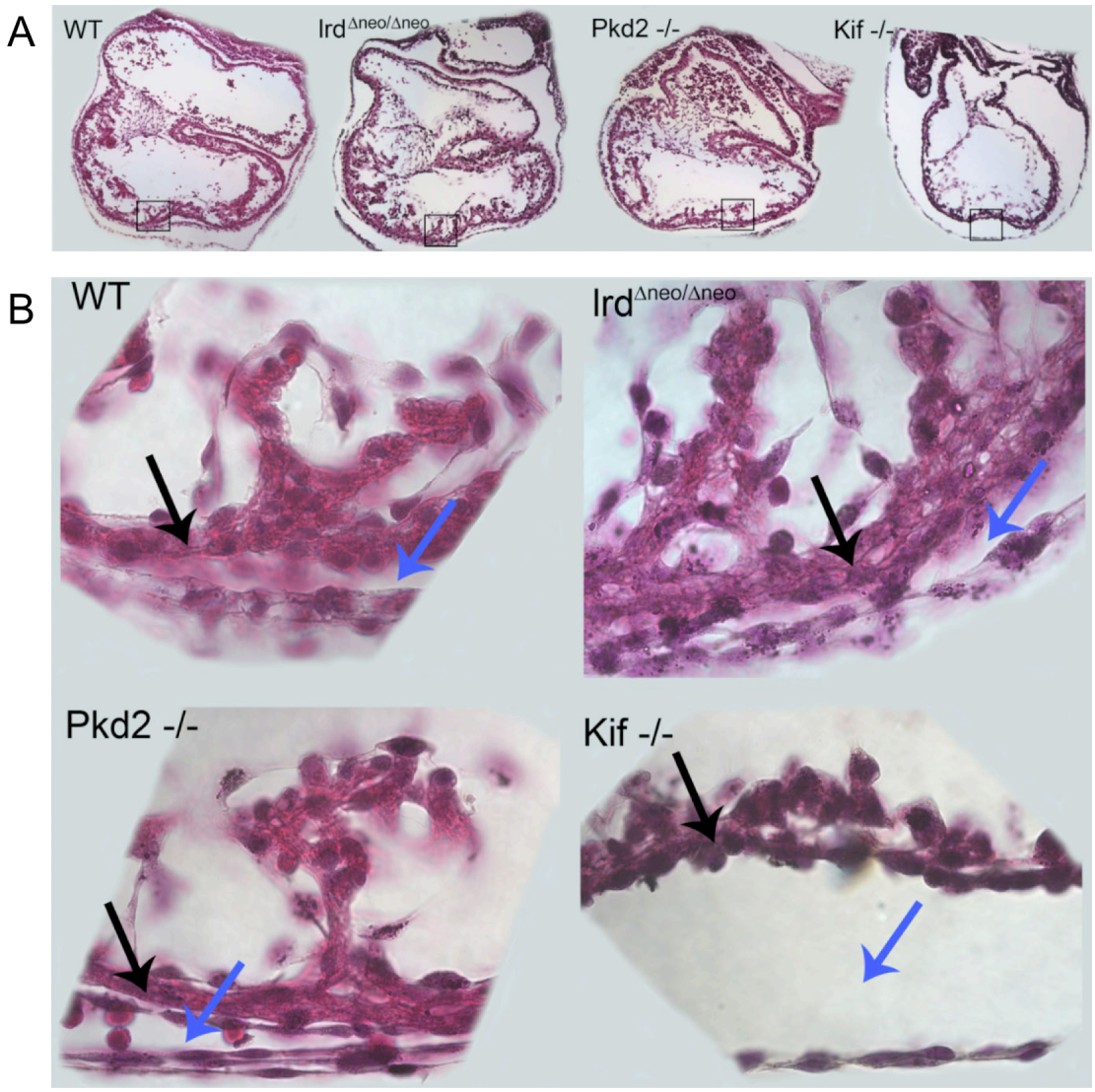

Fig. 9. Magnified view of myocardium in e9.5 wild-type, lrd$^{\Delta neo/\Delta neo}$, Pkd2$^{-/-}$, and Kif3a$^{-/-}$ embryos, stained with hematoxylin and eosin. **A:** Overview. Boxed outline panels enlarged in B. **B:** Magnification of ventricular trabeculations, compact myocardium (black arrow), epicardium, and endocardium. Blue arrow indicates pericardial space.

large pericardial effusion is visible. The CM is rarely more than one cell layer thick and it is difficult to distinguish the flattened epithelial cells of epicardium and endocardium from the myocardial cells.

These results suggest a role for cardiac cilia in the formation of the ECCs and in the development of the CM distinct from the role of cilia in LR development. The most

severe phenotype is seen in mice with a complete absence of cilia suggesting a role for cardiac cilia beyond a Pkd2 mediated sensory role.

Mice with Defective Ciliary Biogenesis Show Upregulation of Gata4 Expression in the Endocardial Cushions.

To determine the changes in *Gata4* transcription in mice lacking cardiac cilia compared to mice with cardiac cilia, we performed whole mount *in situ* hybridization on e9.5 $lrd^{\Delta neo/\ \Delta neo}$ ($lrd^{-/-}$, defective ciliary motility), $Inv^{-/-}$ (unknown defect, cilia present), $Kif3a^{-/-}$ (defective ciliary biogenesis), and $Ift20^{-/-}$ (defective ciliary biogenesis) embryos. We chose to look at *Gata4* expression because mice with homozygous *Gata4* deletions in the developing heart have hypocellular ECCs suggesting a role for *Gata4* in EMT. Frozen sections were obtained and counterstained with nuclear fast red. Although mice at e9.5 were chosen, their true ages varied from e9.0-e9.5. Thus, the mutants are not perfectly matched in terms of age and obtaining more embryos would help us perform more complete comparisons. Mutant mice were paired with homozygous (+/+) or heterozygous (+/-) littermates as wild-type controls.

We observed *Gata4* expression in numerous heart structures including the atria, ventricles, and ECCs (Fig. 10A). In the ECCs, *Gata4* expression is visible in both the mesenchymal and endocardial components (Fig. 10C, arrow indicates mesenchymal cells). In the ventricles, *Gata4* is expressed in the epicardium and both the trabecular and compact myocardium (Fig. 10D).

When comparing *Gata4* expression between cilia-mutant mice and their littermates, we found that both the $lrd^{\Delta neo/\ \Delta neo}$ and the $Inv^{-/-}$ embryos show similar

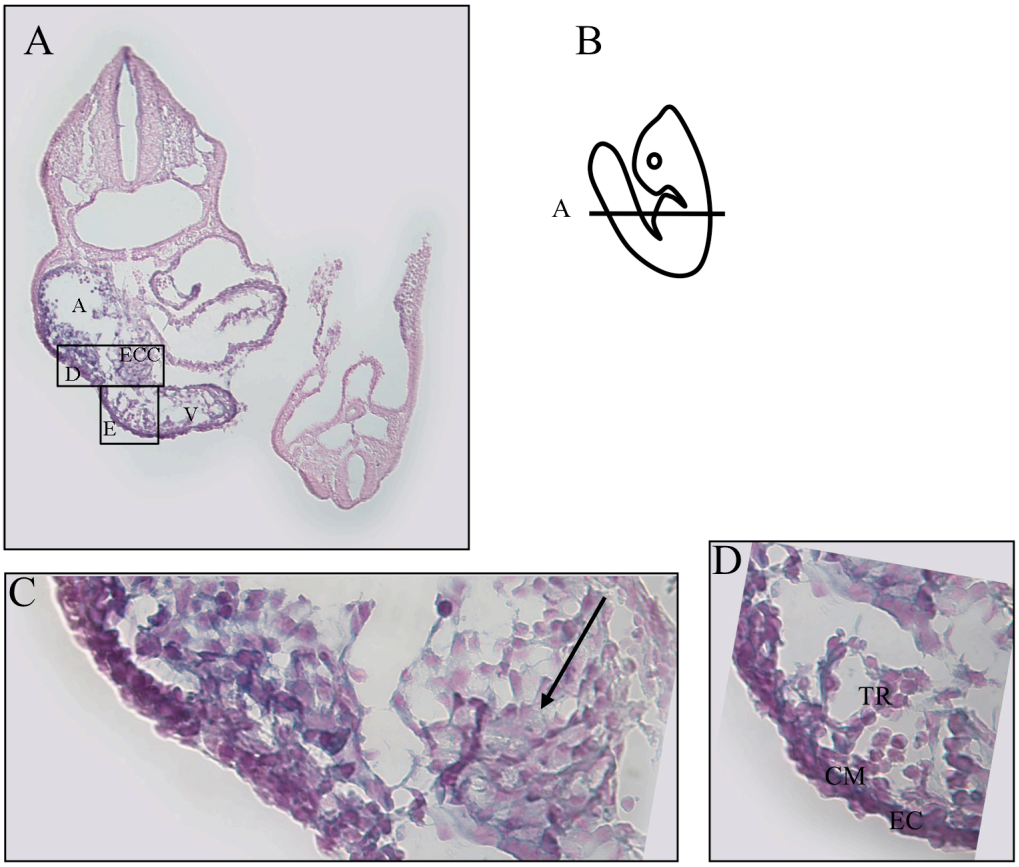

Fig. 10. Expression of *Gata4* in e9.5 wild-type mice. **A:** Overview of embryo showing *Gata4* staining (purple) in atrium (A), ventricle (V), and endocardial cushions (ECC). Boxed outline panels enlarged in C-D. **B:** Diagram showing level of transverse sections. **C:** Magnified view of the ECCs. Arrow indicates mesenchymal cells. **D:** Magnified view of ventricular trabeculations (TR), compact myocardium (CM), and epicardium (EC) showing *Gata4* expression in all cell layers.

expression patterns and signal intensity as the wild-type controls. *Gata4* is expressed throughout the atria, ventricles and ECCs in a pattern indistinguishable from wild-type (Fig. 11A and Fig. 11B). A striking finding was seen in the ECCs of Kif3a$^{-/-}$ and Ift20$^{-/-}$ embryos (Fig. 11C and Fig. 11D). The Kif3a$^{-/-}$ embryo had fewer mesenchymal cells in the ECCs than the Kif3a$^{+/+}$ embryo (Fig. 11D); nevertheless, the ECC endocardial cells have a darker *Gata4* stain than the corresponding cells in the Kif3a$^{+/+}$ embryo (Fig. 11D). The Kif3a$^{-/-}$ embryo also has decreased trabeculations when compared to Kif3a$^{+/+}$;

however,

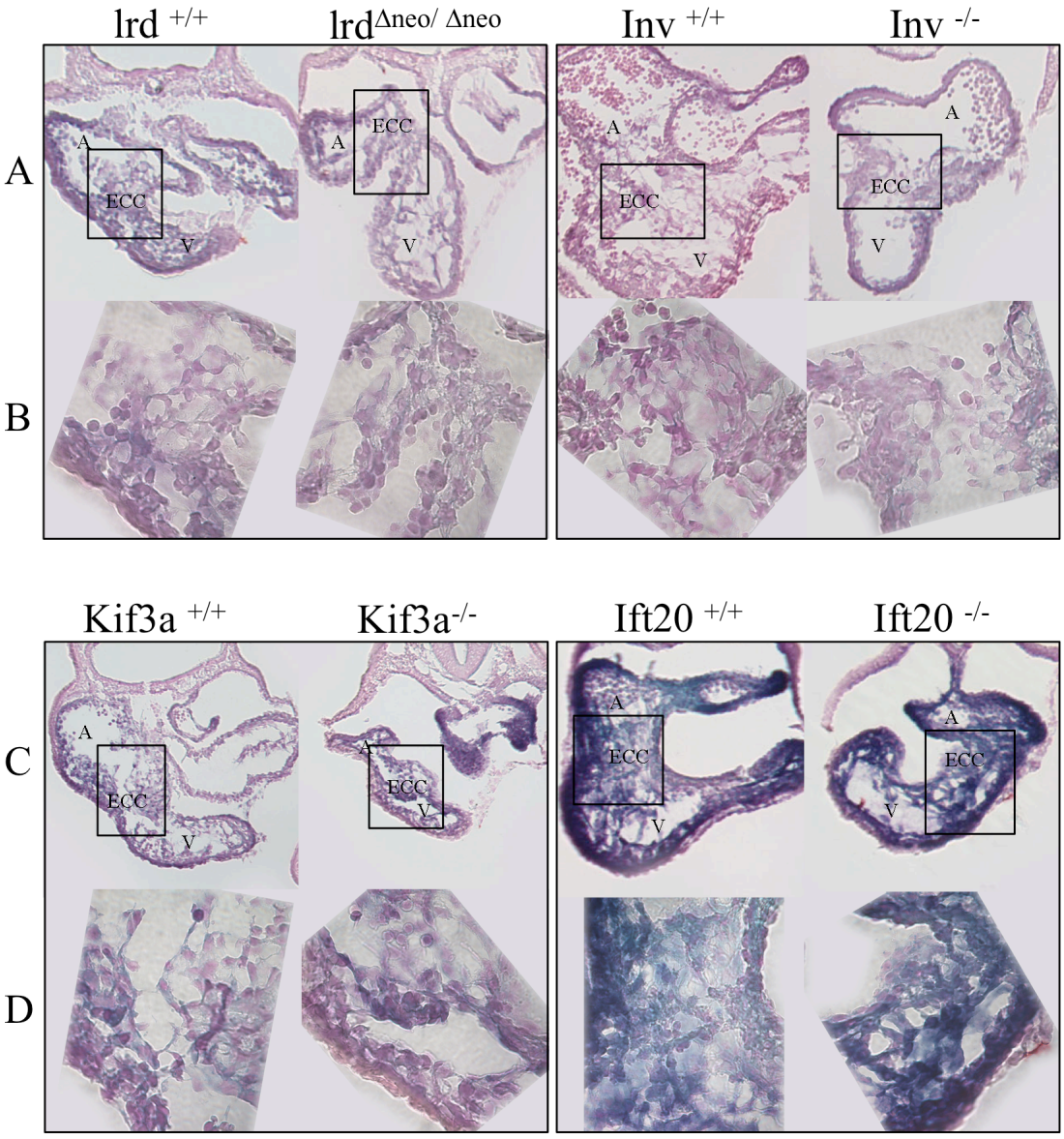

Fig. 11. Expression of *Gata4* in e9.5 wild-type, $lrd^{\Delta neo/\ \Delta neo}$, $Inv^{-/-}$, $Kif3a^{-/-}$, and $Ift20^{-/-}$ embryos. **A:** Overview of lrd $^{+/+}$, $lrd^{\Delta neo/\ \Delta neo}$, $Inv^{+/+,}$ and $Inv^{-/-}$ hearts including atria (A), ventricles (V) and endocardial cushions (ECC). Boxed outline panels enlarged in B. **B:** Magnified view of ECCs showing comparable *Gata4* expression between wild-type and mutant mice. **C:** Overview of $Kif3a^{+/+}$, $Kif3a^{-/-}$, $Ift20^{+/+}$, and $Ift20^{-/-}$ hearts. Boxed outline panels enlarged in D. **D:** Magnified view of ECCs showing increased *Gata4* expression in $Kif3a^{-/-}$ and $Ift20^{-/-}$ embryos.

the degree of *Gata4* staining in the trabecular myocardium is consistent with wild-type (Fig. 11C). *Gata4* expression is also unaffected in the CM and the epicardium (Fig. 11C). Ift20 $^{-/-}$ and Ift20 $^{+/+}$ embryos both have darker overall *Gata4* staining compared to

the other mutant and wild-type embryos (Fig. 11C). This is likely an artifact from embryo harvesting, as all wild-type embryos should be identical. Despite this overall increased intensity, the Ift$^{-/-}$ embryo has similar characteristics to the Kif3a$^{-/-}$ embryo. The Ift20 $^{-/-}$ embryo has fewer mesenchymal cells and increased *Gata4* expression (Fig. 11D) compared to Ift20$^{+/+}$. The CM, trabecular myocardium and epicardium of the Ift20 $^{-/-}$ embryo show unchanged *Gata4* expression compared to Ift20$^{+/+}$ (Fig. 11C).

These results suggest that mice with defects in ciliary biogenesis, such as Kif3a$^{-/-}$ and Ift20 $^{-/-}$, have an upregulation of *Gata4* expression in the ECCs. It is possible that cilia and *Gata4* act as part of a common or parallel pathway during ECC development.

Conclusions and Discussion

Cardiac Defects seen in Mice with Defective Ciliary Biogenesis are due to a Direct Role of Cardiac Cilia on Heart Development.

Heart defects are a significant part of the phenotype described in mice with mutations affecting the formation and function of cilia. Some of these congenital heart defects are secondary to abnormal left-right (LR) development which occurs in the absence of nodal cilia (33). However, we show that the abnormal cardiogenesis observed in mice without cilia extends beyond that of LR development. We demonstrate another subset of cilia, which we call *cardiac cilia*, that are located in the embryonic heart and could play a direct role in cardiac development.

Cardiac Cilia are Present on Key Locations during Important Time Points in Cardiogenesis

Cardiogenesis is a carefully regulated process with many critical steps occurring between e9.5 and e12.5, the time points where we demonstrate the presence of cardiac cilia. At e9.5, the heart has begun contracting and ECC development has been initiated, while by e12.5 the process of EMT is almost complete. During this time, cardiac cilia could sense fluid flow as they do on kidney and embryonic node epithelial cells (32,33) or regulate other signaling pathways known to take place in the cilium (36). Similar to studies on the embryonic chicken heart (39), we observed cilia on the endocardial cells lining the atria, ventricles, and ECCs. In both the chicken and mouse hearts, cilia are visualized either immersed in cytoplasm or protruding from the luminal cell surface. The

orientation of endocardial cilia into the atrioventricular (AV) cavity may enable them to sense blood flow and contribute to developmental signaling pathways.

We observed cilia distribution to be dynamic between time points. Compared to e9.5 mice, the ECCs of e12.5 mice have fewer cilia on the endocardial surfaces, but increased cilia density on the mesenchymal components. Cilia are known to resorb when exposed to increased shear stress *in vitro* (40), supporting these observations. An additional change observed at e12.5 mice, is the presence of a highly ciliated epicardium. These cilia protrude into the pericardial space where, although unable to sense blood flow, they could sense the frictional motion of the epicardium against the pericardium during myocardial contraction.

Cardiac Cilia Function Outside of Left-Right Asymmetry

Given the important role that cilia play in establishing the position of the heart along the LR axis, it was initially thought that the heart defects seen in mice with ciliary mutations were secondary to abnormal LR positioning. To evaluate the possibility that cilia play a more direct role in cardiogenesis, we compared the cardiac phenotypes of mice with mutations affecting ciliary biogenesis, motility, and mechanosensation. We found that the cardiac defects correspond not to the direction of heart looping, but to the characteristics of the underlying ciliary mutations, as all mice compared actually have normal D-looped hearts.

Cardiac Cilia do not Function by Generating Fluid Flow

Of the three ciliary mutant mice we compared, $lrd^{\Delta neo/\Delta neo}$ embryos have the mildest

phenotype. Left-right dynein (lrd) encodes the microtubule-based motor protein responsible for ciliary motility and generation of the leftward nodal flow crucial for LR determination. $lrd^{\Delta neo/\Delta neo}$ embryos have immotile but structurally normal cilia. Although lrd is expressed in the node, neural tube, gut, and limb from e7.5 to e12.5, it is never expressed in the embryonic mouse heart (44). When we examined $lrd^{\Delta neo/\Delta neo}$ mice, we found the cardiac phenotype of D-looped embryos to be grossly comparable to wild-type. Previous studies have demonstrated that 40% of $lrd^{\Delta neo/\Delta neo}$ mice have intracardiac defects including ECC defects, double-outlet RVs, and transposition of the great vessels, but the remaining 60% have normal hearts. The presence of heart defects is not related to the LR patterning as equal numbers of D-looped and L-looped hearts had cardiac malformations (49). Because lrd is not expressed in the mouse heart and deletion of this protein does not lead to a severe cardiac phenotype, we conclude that cardiac cilia do not function via a lrd mediated generation of fluid flow.

Cardiac Cilia do not Function Solely by a Pkd2-Mediated Sensory Role

The most severe cardiac phenotypes are seen in $Pkd2^{-/-}$ and $Kif3a^{-/-}$ mouse embryos. Pkd2 encodes the calcium release channel, polycystin-2, present in the heart from e8.5 to e15.5 (55). Pkd2 has been implicated in a mechanosensory role in kidney cells (32) as well as the embryonic node, where it may sense the increased intracellular calcium concentration generated by lrd mediated leftward nodal flow (33). We demonstrate that although $Pkd2^{-/-}$ mouse hearts show abnormal cardiac development, their phenotype is not as severe as $Kif3a^{-/-}$ mice. $Kif3a^{-/-}$ embryonic mouse hearts have no mesenchymal cells in the ECCs, decreased ventricular trabeculations, and a thinned

compact myocardium (CM). These mice lack the ubiquitously expressed Kif3a motor subunit of the kinesin-II motor complex. This complex is involved in intraflagellar transport (IFT) necessary for ciliary biogenesis and thus Kif3a$^{-/-}$ mice have no cilia (46). If the role of cardiac cilia were confined to a polycystin-2 mediated sensory role, we would expect Pkd2$^{-/-}$ and Kif3a$^{-/-}$ mice to exhibit similar phenotypes, as Kif3a$^{-/-}$ mice have no cilia and thus no Pkd2 signaling. Because the cardiac phenotype in mice without cilia is more severe, this suggests a role for cardiac cilia beyond any Pkd2-mediated mechanosensory role. The cardiac cilia could still function to sense fluid flow, but by using an as of yet undetermined method of signal transmission.

Cardiac Cilia Function in EMT and the Formation of the Compact Myocardium

The Role of Cilia and the Cytoskeleton in Mechanosensation

Fluid flow has been shown to be important in early cardiogenesis and disruptions in this flow cause numerous cardiac defects. The cardiovascular malformations seen in the chicken venous clip model and mice with absent fluid flow are due to abnormal ECC development or lack of EMT (29,30). These phenotypes are reminiscent of the phenotypes we observe in our mice without cardiac cilia and suggest of a role for cilia in mediating the effects of fluid flow on ECC development. Cardiac cilia protrude into the cardiac lumen, positioning them in a location where they could detect changes in local shear forces. Primary cilia from cultured kidney cells have been shown to bend reversibly to large angles when exposed to fluid flow (56) and ciliated CHEC cells respond to such flow by increasing the transcription of shear stress proteins (41). The

basal body connects cilia to the cytoskeleton (57), an expansive network of microtubules, actin microfilaments, and intermediate filaments (58), providing a structure through which the signals received by cilia could be integrated. Interestingly other molecules implicated as potential fluid shear stress sensors, such as integrins, cell-cell adhesion molecules, ion channels, receptor tyrosine kinases, and G protein coupled receptors are all directly or indirectly linked to the cytoskeleton (31,59). The importance of the cytoskeleton in this pathway is emphasized in experiments demonstrating a decreased cellular response to shear stress after disruption of cytoskeletal microtubules. The converse is also true with microtubule stabilization leading to an increased response to fluid shear stress (41). Together, this data suggests a model where the bending of cilia in response to fluid flow may lead to cytoskeletal deformation and the activation of any number of downstream signaling targets.

A Model for Cardiac Cilia in EMT

In vitro studies have shown a direct correlation between the presence of cilia and the expression of shear stress proteins in response to fluid flow (41). However, *in vivo* studies in the embryonic chicken heart show that during late cardiogenesis there is an inverse relationship between the magnitude of shear stress and the density of cilia. Monocilia were visible on areas of low shear stress such as the upstream and downstream portions of the AV cushions, but no monocilia were detected on the endocardial cells lining the narrowest passage of the AV canal, a region exposed to higher fluid flow (39). Cilia on HUVEC cells disassemble when exposed to high laminar shear stress (40).

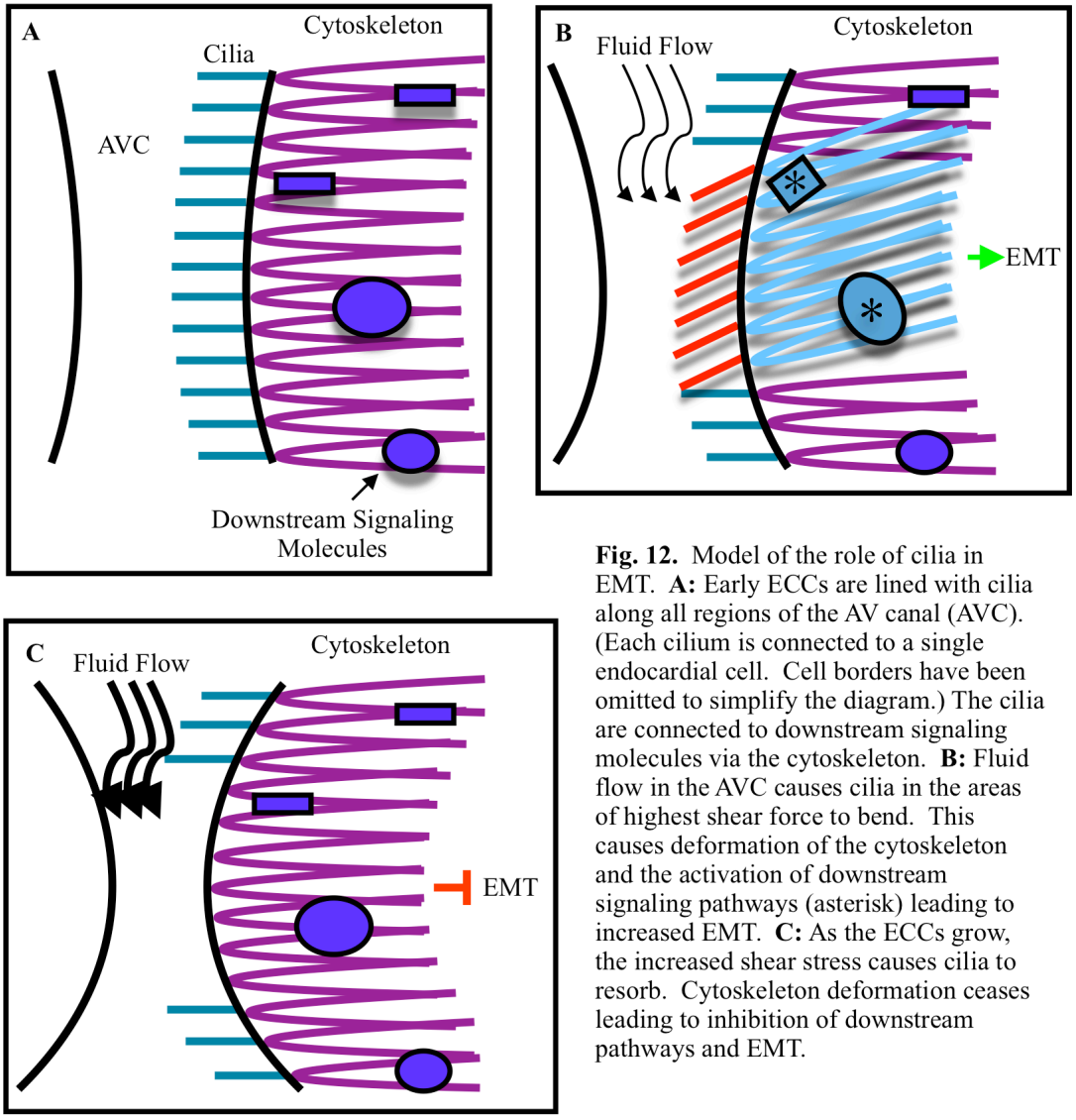

Fig. 12. Model of the role of cilia in EMT. **A:** Early ECCs are lined with cilia along all regions of the AV canal (AVC). (Each cilium is connected to a single endocardial cell. Cell borders have been omitted to simplify the diagram.) The cilia are connected to downstream signaling molecules via the cytoskeleton. **B:** Fluid flow in the AVC causes cilia in the areas of highest shear force to bend. This causes deformation of the cytoskeleton and the activation of downstream signaling pathways (asterisk) leading to increased EMT. **C:** As the ECCs grow, the increased shear stress causes cilia to resorb. Cytoskeleton deformation ceases leading to inhibition of downstream pathways and EMT.

These findings support the function of cilia in a two-step model (Fig. 12). First, early in development, cilia are present on all surfaces of the ECCs (Fig.12A) where we suggest they may function to sense localized shear forces and contribute to the progression of EMT. The signal transmission could be propagated through connections with the cytoskeleton (Fig. 12B). As EMT progresses and the ECCs expand, the AV canal narrows leading to an increase in local shear forces. We hypothesize that this high shear stress causes the cilia on the endocardial cells lining the AV canal to disassemble and

EMT to be inhibited (Fig. 12C). In this model, cilia function both to promote EMT during cushion growth and then to inhibit EMT after the ECCs have grown to the appropriate size. If cilia are not present to sense fluid flow or fluid flow is not established, the signal to promote EMT will be missing and mesenchymal cells will not populate the cardiac jelly. This phenotype of hypocellular ECCs is one that we observe in our mice with absent cilia.

Cardiac Cilia Promote Myocardial Proliferation

In addition to changes in the ECCs, we observed that Kif3a$^{-/-}$ mice have a thinned compact myocardium (CM). In wild-type mice, cilia are located on the atrial and ventricular endocardium oriented toward the luminal space. These cilia could sense fluid flow and send a signal to the myocardium to proliferate in much the same way as we hypothesize that ECC cilia function in promoting ECC development. We also observed a cilium protruding from each epicardial cell. These cilia could not sense blood flow within the heart, but as they extend into the pericardial space, they could sense the sliding of the epicardium against the pericardium during contraction. Other studies have shown that the pericardium can be involved in myocardial development. For example, mice with a targeted deletion of Wt-1 exhibit a thinned myocardium despite the expression of Wt-1 solely in the pericardium and not the myocardium (60).

Could Cardiac Cilia Mediate Heart Development through Sonic Hedgehog Signaling?

Cilia have been implicated in a number of signaling pathways including those with hedgehog (Hh), a secreted protein which regulates numerous developmental pathways. The link between cilia and Hh was first noted using studies which showed that mice with mutations in IFT proteins, including Kif3a, failed to properly activate downstream targets of sonic hedgehog (Shh), one of three mammalian hedgehog genes (61). It has since been demonstrated that numerous components of this pathway localize to the cilium (62,63). Interestingly, $Kif3a^{-/-}$ embryos exhibit a similar phenotype as mice with mutations in the protein Smoothened (Smo), a downstream component of the Hh pathway (64). At e8.0, $Smo^{-/-}$ mice also have decreased expression of Nkx2.5, a transcription factor involved in specifying early myocardial lineage, suggesting that Shh signaling controls early Nkx2.5 expression (64,65). Mice with an over-expression of Nkx2.5 and those with increased Hh signaling secondary to a mutation in suppressor of fused (SuFu) a negative regulator of Hh signaling, both have myocardial hyperplasia (65,66). Conversely, Nkx2.5 knockout mice have myocardial thinning (67). Together this data supports a model where cardiac cilia function in mediating Shh signaling and the activation of Smo (Fig. 13). Smo activation then leads to downstream activation of Nkx2, which exerts its effects on myocardial proliferation. In the absence of cilia, these molecules could not colocalize, the signals could not be propagated, and the mice would have myocardial thinning, the phenotype we observe in our mice without cilia. In this

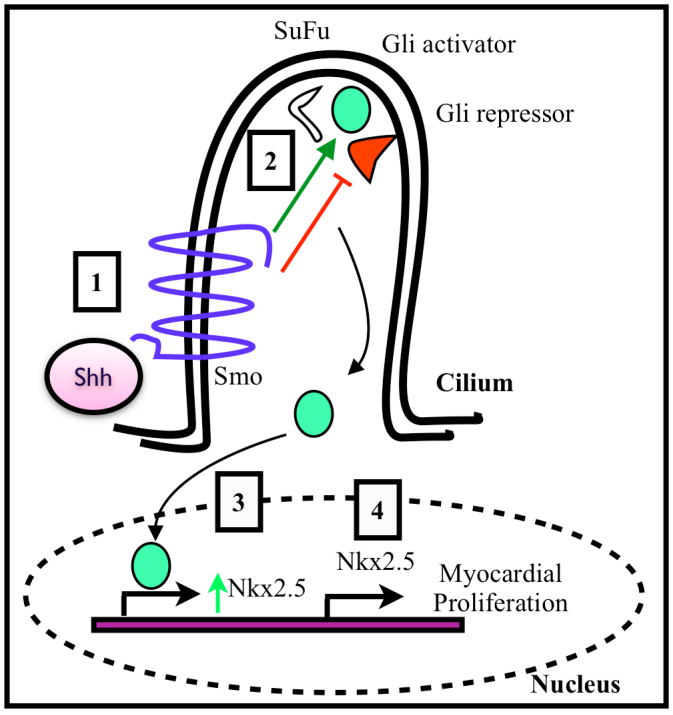

Fig 13. Model for cilia and Shh in myocardial proliferation. **1:** In the presence of Shh, smoothened (Smo) is activated. **2:** This releases the inhibition of Suppressor of Fused (SuFu) on the downstream Shh activator (Gli). **3:** Gli translocates to the nucleus where it increases transcription of genes including Nkx2.5. **4:** Nkx2.5 in turn increases transcription of genes involved in myocardial proliferation

model, cilia are important in promoting and/or regulating myocardial proliferation via the sonic hedgehog pathway.

$Shh^{-/-}$ mice have abnormal outflow tract development (68) as well as atrioventricular septal defects (AVSD) (69). However, these AVSDs are thought to arise from abnormal development of the dorsal mesocardium rather than the ECCs. In fact, $Shh^{-/-}$ mice demonstrate normal AV cushion formation and growth from e9.5 to e11.5 (70), the time frame where we see our phenotypes first emerge. If loss of cilia-mediated Shh signaling was responsible for the hypocellular ECCs we observed in our mice, we would expect $Shh^{-/-}$ mice to have similar ECC defects. Normal AV cushions in $Shh^{-/-}$ mice suggest that although it is possible that cilia could regulate proliferation of the CM via hedgehog signaling, cilia do not mediate EMT in the ECCs via this pathway alone.

Cilia Affect the Expression Pattern of the Transcription Factor Gata4

Gata4 is Expressed in the Developing Heart

In this work, we confirm the expression pattern of *Gata4*, a zinc finger transcription factor which is essential for heart formation. In e9.5 wild-type mice, *Gata4* expression is observed in the endocardium lining the cardiac chambers and ECCs as well as in the ventricular myocardium and epicardium, a distribution which is supported by previous work (23,24). Interestingly, these areas correspond to regions of the heart where we identified cilia.

Gata4 Expression is Upregulated in Mice without Cilia

Given that neither mutants with an endothelial restricted activation of Gata4 ($Gata4^{T2del}$) nor our mice without cardiac cilia can undergo EMT, it is possible that Gata4 and cilia function in a common or parallel pathway. To determine the effect of cilia on *Gata4* expression patterns, we compared four mouse embryos with different mutations affecting ciliary synthesis or function. We found that the results stratified into two different groups. The first included $Inv^{-/-}$ and $lrd^{\Delta neo/\Delta neo}$ embryos, which appeared to have similar *Gata4* expression compared to wild-type embryos. Although the function of the protein disrupted in $Inv^{-/-}$ mice is unknown, all $Inv^{-/-}$ mice are *situs inversus* (48). We previously demonstrated that $lrd^{\Delta neo/\Delta neo}$ embryos, which have randomized LR development, have a similar phenotype to wild-type mice and concluded first that cardiac cilia function in a role outside of LR development and second that they do not function via a lrd-mediated role. Given that Inv's sole function is also in LR development and that $Inv^{-/-}$ embryos have a normal cardiac phenotype, we would expect these mutants to

behave similarly to $Ift^{\Delta neo/\Delta neo}$ embryos. The normal *Gata4* expression pattern that we have observed continues to support the theory that the role of cardiac cilia is beyond that of LR development.

In contrast to $Inv^{-/-}$ and $lrd^{\Delta neo/\Delta neo}$ embryos, we found that $Kif3a^{-/-}$ and $Ift20^{-/-}$ embryos have upregulated *Gata4* expression in the ECCs. These mice have no cilia secondary to failure of intraflagellar transport (IFT): $Kif3a^{-/-}$ because of a defect in a motor subunit of the kinesin-II complex and $Ift20^{-/-}$ because of a mutation in the IFT20 subunit of the IFT particle. It has been shown that a knockout of IFT20 blocks ciliary assembly (45). Other heart structures such as the ventricular trabeculations, compact myocardium, and epicardium appear to have comparable *Gata4* expression to wild-type mice. This suggests that the interaction between Gata4 and cardiac cilia is limited to the ECCs.

Cilia and Gata4 may Function in a Common or Parallel Pathway to Promote EMT

Our work shows that cilia affect levels of the transcription factor Gata4 as evidenced by Gata4 upregulation in mice without cardiac cilia. Gata4 has been shown to function upstream of a complex signaling pathway necessary for EMT. In the absence of Gata4 or any member of the ErbB-Ras-Erk pathway, the ECCs are not seeded with mesenchymal cells (15,20,21,27). This phenotype of hypocellular ECCs is identical to what we observe in our $Kif^{-/-}$ mice, which lack cardiac cilia. Given that cilia can affect levels of Gata4 and that mice with mutations in Gata4 or proteins involved in ciliary biogenesis have hypocellular cushions, cilia and Gata4 may work in the same or a parallel pathway to promote EMT.

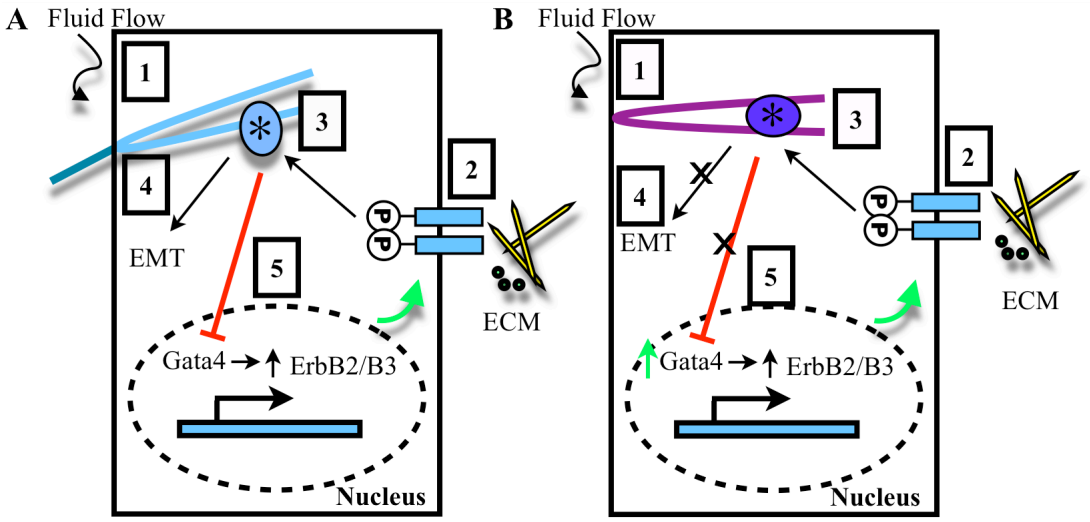

Fig. 14. Model where Gata4 and cilia function in the same pathway.
A-B: Endocardial cell in the AV canal during high fluid flow.
A: Cilia present. **1:** Cilia sense shear stress and connect to downstream signaling pathways (asterisk) via the cytoskeleton. **2:** The ErbB2/B3 pathway is concurrently initiated via interactions with ECM components. **3:** The two pathways converge at any downstream Erb signaling molecule (asterisk) including Ras, MEK, or Erk via cytoskeletal interactions. **4:** EMT is promoted. **5:** Gata4 functions to increase transcription of ErbB2/B3 (green arrow), while a negative feedback loop keeps Gata4 expression in check (red arrow).
B: Cilia are absent. **1:** Cilia are not present to sense fluid flow. Absence of cytoskeletal deformation prevents activation of downstream signaling pathways (asterisk). **2:** The ErbB2/B3 pathway is still initiated. **3:** The two pathways converge but without the signal from cilia, the common downstream signaling pathway does not progress. **4:** EMT is inhibited. **5:** The negative feedback loop on Gata4 does not function allowing Gata4 expression to increase uninhibited.

If cilia and Gata4 functioned in the same pathway (Fig. 14), then in order to increase Gata4 levels, cilia must act downstream of Gata4. This could occur at any point along the ErbB-Ras-Erk pathway (Fig. 14A). In the absence of cilia (Fig 14B), the Erb pathway would not function leading to a decreased concentration of all of the downstream signaling molecules. In addition, this could lead to the inhibition of a negative feedback loop on Gata4 allowing Gata4 expression to increase unchecked, the phenotype we observe in our mice without cilia. Although ErbB2/ErbB3, Ras, and Erk have not been shown to interact with cilia per se, tyrosine kinase receptors, G proteins, and numerous other kinases are linked to the cytoskeleton (31,59), making it possible that cilia influence this pathway via cytoskeletal interactions.

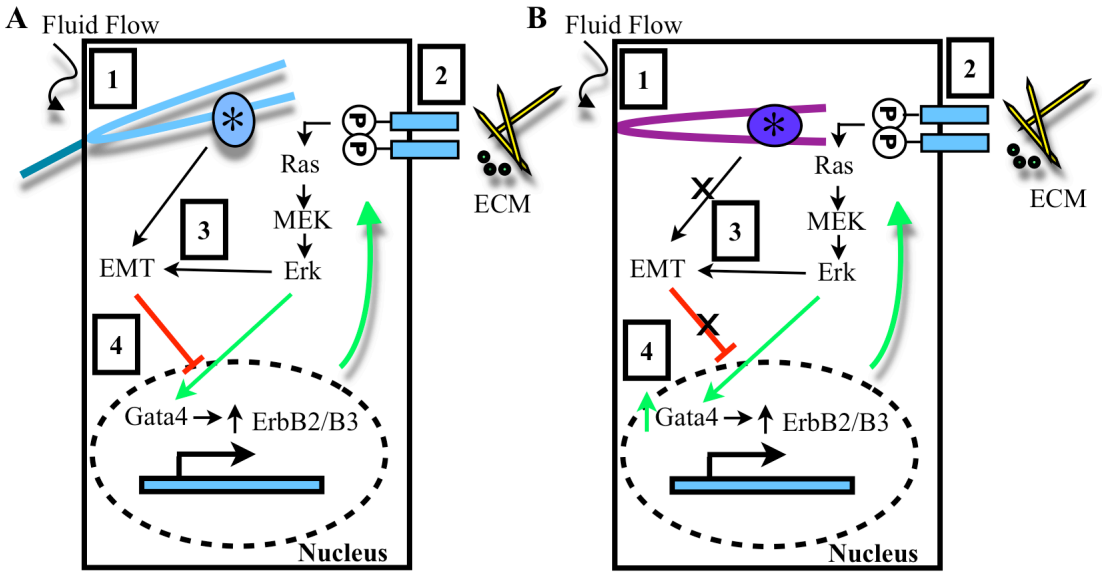

Fig. 15. Model where Gata4 and cilia function in parallel pathways.
A-B: Endocardial cell in the AV canal during high fluid flow.
A: Cilia present. **1:** Cilia sense shear stress and connect to downstream signaling pathways (asterisk) via the cytoskeleton. **2:** The ErbB2/B3 pathway is concurrently initiated via interactions with ECM components. **3:** The two pathways independently lead to EMT: cilia via cytoskeletal deformation and unknown downstream signaling molecules and Erb via the Ras-MEK-Erk pathway. **4:** Erk functions as a positive regulator of Gata4 to increase Erb transcription (green arrows), while a negative feedback loop keeps Gata4 expression under control (red arrow).
B: Cilia are absent. **1:** Cilia are not present to sense fluid flow. Absence of cytoskeletal deformation prevents activation of downstream signaling pathways (asterisk). **2:** The ErbB2/B3 pathway is still initiated and proceeds normally. **3:** The Erb pathway promotes EMT, but without signals from the cilia pathway, EMT is not initiated. **4:** The negative feedback loop on Gata4 does not function. This allows the Erk positive feedback look to go unchecked and Gata4 expression to increase uninhibited.

Interestingly, in *in vivo* studies of rat cardiomyocytes, Erk has been shown to enhance the transcriptional potency of Gata4 through phosphorylation (71). Although this has not been studied during embryogenesis, if Erk did function as a positive regulator of Gata4, this could support the idea that cilia function parallel to the Gata4-Erb-Ras-Erk pathway (Fig.15). In this model, both the Gata4-mediated pathway and the cilia-mediated pathway separately lead to EMT. Both pathways are necessary but not sufficient for EMT as defects in either can independently lead to ECC defects. In wild-type mice (Fig. 15A), the Erk-Gata4 positive feedback loop would function to continually stimulate Gata4 to increase ErbB3 transcription and thus to continue EMT. When EMT

is complete, a downstream molecule then participates in a negative feedback loop on either Gata4 or Erk to decrease Gata4 levels and thus ErbB3 transcription. In the absence of cilia (Fig15B), and thus EMT, the negative feedback loop is never activated leaving the Erk-Gata4 positive feedback loop functioning to continually increase Gata4 levels.

We hypothesize that cilia function as shear stress sensors and promote EMT through interactions with the cytoskeleton and downstream signaling molecules. We propose that a parallel pathway model is more likely. In this model, the endocardium responds to myocardial signals through pathways like the ErbB-Ras-Erk pathway. This is necessary for EMT, but not sufficient as a second signal, one from the intraluminal cilia which signal the presence of fluid flow in the heart, must also be present for EMT to proceed.

Future Directions

Together these results suggest a direct role for cardiac cilia in heart development by demonstrating the presence of cilia on key locations of the embryonic heart, by characterizing the phenotype of mice without cilia, and by showing that cilia affect the expression of a transcription factor known to be involved in EMT.

More work should be done to further characterize the role that cardiac cilia play in heart development. We hypothesize that cilia are involved in both EMT and the formation of the CM. Selective inactivation of cilia in different locations could help confirm which cilia are responsible for which phenotypes. For example, does targeted deletion of cilia on the epicardium lead to a thinned myocardium? It would also be useful to examine the phenotype of mice with a mutation that hindered cilia from disassembling

in response to shear stress. If cilia function to promote EMT and their absence leads to EMT inhibition, we would expect constituently expressed cilia to lead to hypercellular ECCs.

It is necessary to further characterize the possible interactions between cilia and the Gata4 pathway. First, quantitative PCR of Gata4 expression on wild-type mice and mice without cilia would help quantify the degree of Gata4 upregulation. Second, we could perform *in situ* hybridization with ErbB3, Ras, and Erk to look for expression patterns in the ECCs of cilia mutant mice. Third, to determine whether cilia function upstream or downstream of Ras, mice without cilia could be infected with a constitutively active Ras. If cilia function upstream of Ras, we would expect this to rescue the cardiac cushion defect, whereas if cilia function downstream of Ras, the mice would continue to have hypocellular ECCs.

References

1. Pierpont ME, Markwald RR, Lin AE. Genetic aspects of atrioventricular septal defects. Am J Med Genet 2000;97:289-96.

2. Armstrong EJ, Bischoff J. Heart valve development: endothelial cell signaling and differentiation. Circ Res 2004;95:459-70.

3. Person AD, Klewer SE, Runyan RB. Cell biology of cardiac cushion development. Int Rev Cytol 2005;243:287-335.

4. Manner J. The anatomy of cardiac looping: a step towards the understanding of the morphogenesis of several forms of congenital cardiac malformations. Clin Anat 2009;22:21-35.

5. Chang C. On the reaction of the endocardium to the bloodstream in the embryonic heart, with special reference to the endocardial thickenings in the atrioventricular canal and the bulbis coris. Ant Rec 1932;:253-65.

6. Patten BM, Kramer TC, and Barry A. Valvular action in the embryonic chick heart by localized apposition of the endocardial masses. Ant Rec 1948;:299-311.

7. Kinsella MG, Fitzharris TP. Origin of cushion tissue in the developing chick heart: cinematographic recordings of in situ formation. Science 1980;207:1359-60.

8. Kalluri R, Weinberg RA. The basics of epithelial-mesenchymal transition. J Clin Invest 2009;119:1420-8.

9. Mjaatvedt CH, Lepera RC, Markwald RR. Myocardial specificity for initiating endothelial-mesenchymal cell transition in embryonic chick heart correlates with a particulate distribution of fibronectin. Dev Biol 1987;119:59-67.

10. Runyan RB, Markwald RR. Invasion of mesenchyme into three-dimensional collagen gels: a regional and temporal analysis of interaction in embryonic heart tissue. Dev Biol 1983;95:108-14.

11. Bernanke DH, Markwald RR. Migratory behavior of cardiac cushion tissue cells in a collagen-lattice culture system. Dev Biol 1982;91:235-45.

12. Potts JD, Runyan RB. Epithelial-mesenchymal cell transformation in the embryonic heart can be mediated, in part, by transforming growth factor beta. Dev Biol 1989;134:392-401.

13. Sugi Y, Yamamura H, Okagawa H, Markwald RR. Bone morphogenetic protein-2 can mediate myocardial regulation of atrioventricular cushion mesenchymal cell formation in mice. Dev Biol 2004;269:505-18.

14. Nieto MA, Sargent MG, Wilkinson DG, Cooke J. Control of cell behavior during vertebrate development by Slug, a zinc finger gene. Science 1994;264:835-9.

15. Camenisch TD, Spicer AP, Brehm-Gibson T, et al. Disruption of hyaluronan synthase-2 abrogates normal cardiac morphogenesis and hyaluronan-mediated transformation of epithelium to mesenchyme. J Clin Invest 2000;106:349-60.

16. Dor Y, Klewer SE, McDonald JA, Keshet E, Camenisch TD. VEGF modulates early heart valve formation. Anat Rec A Discov Mol Cell Evol Biol 2003;271:202-8.

17. Enciso JM, Gratzinger D, Camenisch TD, Canosa S, Pinter E, Madri JA. Elevated glucose inhibits VEGF-A-mediated endocardial cushion formation: modulation by PECAM-1 and MMP-2. J Cell Biol 2003;160:605-15.

18. Pinter E, Haigh J, Nagy A, Madri JA. Hyperglycemia-induced vasculopathy in the murine conceptus is mediated via reductions of VEGF-A expression and VEGF receptor activation. Am J Pathol 2001;158:1199-206.

19. Erickson SL, O'Shea KS, Ghaboosi N, et al. ErbB3 is required for normal cerebellar and cardiac development: a comparison with ErbB2-and heregulin-deficient mice. Development 1997;124:4999-5011.

20. Rivera-Feliciano J, Lee KH, Kong SW, et al. Development of heart valves requires Gata4 expression in endothelial-derived cells. Development 2006;133:3607-18.

21. Camenisch TD, Schroeder JA, Bradley J, Klewer SE, McDonald JA. Heart-valve mesenchyme formation is dependent on hyaluronan-augmented activation of ErbB2-ErbB3 receptors. Nat Med 2002;8:850-5.

22. Meyer D, Birchmeier C. Multiple essential functions of neuregulin in development. Nature 1995;378:386-90.

23. Charron F, Nemer M. GATA transcription factors and cardiac development. Semin Cell Dev Biol 1999;10:85-91.

24. Heikinheimo M, Scandrett JM, Wilson DB. Localization of transcription factor GATA-4 to regions of the mouse embryo involved in cardiac development. Dev Biol 1994;164:361-73.

25. Schultheiss TM, Burch JB, Lassar AB. A role for bone morphogenetic proteins in the induction of cardiac myogenesis. Genes Dev 1997;11:451-62.

26. Garg V, Kathiriya IS, Barnes R, et al. GATA4 mutations cause human congenital heart defects and reveal an interaction with TBX5. Nature 2003;424:443-7.

27. Lakkis MM, Epstein JA. Neurofibromin modulation of ras activity is required for normal endocardial-mesenchymal transformation in the developing heart. Development 1998;125:4359-67.

28. Hogers B, DeRuiter MC, Gittenberger-de Groot AC, Poelmann RE. Unilateral vitelline vein ligation alters intracardiac blood flow patterns and morphogenesis in the chick embryo. Circ Res 1997;80:473-81.

29. Hogers B, DeRuiter MC, Gittenberger-de Groot AC, Poelmann RE. Extraembryonic venous obstructions lead to cardiovascular malformations and can be embryolethal. Cardiovasc Res 1999;41:87-99.

30. Koushik SV, Wang J, Rogers R, et al. Targeted inactivation of the sodium-calcium exchanger (Ncx1) results in the lack of a heartbeat and abnormal myofibrillar organization. FASEB J 2001;15:1209-11.

31. Resnick N, Yahav H, Shay-Salit A, et al. Prog Biophys Mol Biol 2003;81:177-99.

32. Praetorius HA, Spring KR. Bending the MDCK cell primary cilium increases intracellular calcium. J Membr Biol 2001;184:71-9.

33. McGrath J, Somlo S, Makova S, Tian X, Brueckner M. Two populations of node monocilia initiate left-right asymmetry in the mouse. Cell 2003;114:61-73.

34. Wong SY, Reiter JF. The primary cilium at the crossroads of mammalian hedgehog signaling. Curr Top Dev Biol 2008;85:225-60.

35. Davis EE, Brueckner M, Katsanis N. The emerging complexity of the vertebrate cilium: new functional roles for an ancient organelle. Dev Cell 2006;11:9-19.

36. Berbari NF, O'Connor AK, Haycraft CJ, Yoder BK. The primary cilium as a complex signaling center. Curr Biol 2009;19:R526-35.

37. Briffeuil P, Thibaut-Vercruyssen R, Ronveaux-Dupal MF. Ciliation of bovine aortic endothelial cells in culture. Atherosclerosis 1994;106:75-81.

38. Bystrevskaya VB, Lichkun VV, Antonov AS, Perov NA. An ultrastructural study of centriolar complexes in adult and embryonic human aortic endothelial cells. Tissue Cell 1988;20:493-503.

39. Van der Heiden K, Groenendijk BC, Hierck BP, et al. Monocilia on chicken embryonic endocardium in low shear stress areas. Dev Dyn 2006;235:19-28.

40. Iomini C, Tejada K, Mo W, Vaananen H, Piperno G. Primary cilia of human endothelial cells disassemble under laminar shear stress. J Cell Biol 2004;164:811-7.

41. Hierck BP, Van der Heiden K, Alkemade FE, et al. Primary cilia sensitize endothelial cells for fluid shear stress. Dev Dyn 2008;237:725-35.

42. Moyer JH, Lee-Tischler MJ, Kwon HY, et al. Candidate gene associated with a mutation causing recessive polycystic kidney disease in mice. Science 1994;264:1329-33.

43. Afzelius BA. A human syndrome caused by immotile cilia. Science 1976;193:317-9.

44. Supp DM, Brueckner M, Kuehn MR, et al. Targeted deletion of the ATP binding domain of left-right dynein confirms its role in specifying development of left-right asymmetries. Development 1999;126:5495-504.

45. Follit JA, Tuft RA, Fogarty KE, Pazour GJ. The intraflagellar transport protein IFT20 is associated with the Golgi complex and is required for cilia assembly. Mol Biol Cell 2006;17:3781-92.

46. Marszalek JR, Ruiz-Lozano P, Roberts E, Chien KR, Goldstein LS. Situs inversus and embryonic ciliary morphogenesis defects in mouse mutants lacking the KIF3A subunit of kinesin-II. Proc Natl Acad Sci U S A 1999;96:5043-8.

47. Wu G, Markowitz GS, Li L, et al. Cardiac defects and renal failure in mice with targeted mutations in Pkd2. Nat Genet 2000;24:75-8.

48. Yokoyama T, Copeland NG, Jenkins NA, Montgomery CA, Elder FF, Overbeek PA. Reversal of left-right asymmetry: a situs inversus mutation. Science 1993;260:679-82.

49. Icardo JM, Sanchez de Vega MJ. Spectrum of heart malformations in mice with situs solitus, situs inversus, and associated visceral heterotaxy. Circulation 1991;84:2547-58.

50. Tan CH, Tay KH, Sheah K, et al. Perioperative endovascular internal iliac artery occlusion balloon placement in management of placenta accreta. AJR Am J Roentgenol 2007;189:1158-63.

51. Kennedy MP, Omran H, Leigh MW, et al. Congenital heart disease and other heterotaxic defects in a large cohort of patients with primary ciliary dyskinesia. Circulation 2007;115:2814-21.

52. Nonaka S, Tanaka Y, Okada Y, et al. Randomization of left-right asymmetry due to loss of nodal cilia generating leftward flow of extraembryonic fluid in mice lacking KIF3B motor protein. Cell 1998;95:829-37.

53. Wu G, Markowitz GS, Li L, et al. Cardiac defects and renal failure in mice with targeted mutations in Pkd2. Nat Genet 2000;24:75-8.

54. Lowe LA, Kuehn MR. Whole mount in situ hybridization to study gene expression during mouse development. Methods Mol Biol 2000;137:125-37.

55. Guillaume R, Trudel M. Distinct and common developmental expression patterns of the murine Pkd2 and Pkd1 genes. Mech Dev 2000;93:179-83.

56. Schwartz EA, Leonard ML, Bizios R, Bowser SS. Analysis and modeling of the primary cilium bending response to fluid shear. Am J Physiol 1997;272:F132-8.

57. Gordon RE, Lane BP, Miller F. Identification of contractile proteins in basal bodies of ciliated tracheal epithelial cells. J Histochem Cytochem 1980;28:1189-97.

58. Fuchs E, Karakesisoglou I. Bridging cytoskeletal intersections. Genes Dev 2001;15:1-14.

59. Helmke BP, Davies PF. The cytoskeleton under external fluid mechanical forces: hemodynamic forces acting on the endothelium. Ann Biomed Eng 2002;30:284-96.

60. Kreidberg JA, Sariola H, Loring JM, et al. WT-1 is required for early kidney development. Cell 1993;74:679-91.

61. Huangfu D, Liu A, Rakeman AS, Murcia NS, Niswander L, Anderson KV. Hedgehog signaling in the mouse requires intraflagellar transport proteins. Nature 2003;426:83-7.

62. Wang N, Miao H, Li YS, et al. Shear stress regulation of Kruppel-like factor 2 expression is flow pattern-specific. Biochem Biophys Res Commun 2006;341:1244-51.

63. Corbit KC, Aanstad P, Singla V, Norman AR, Stainier DY, Reiter JF. Vertebrate Smoothened functions at the primary cilium. Nature 2005;437:1018-21.

64. Zhang XM, Ramalho-Santos M, McMahon AP. Smoothened mutants reveal redundant roles for Shh and Ihh signaling including regulation of L/R symmetry by the mouse node. Cell 2001;106:781-92.

65. Cleaver OB, Patterson KD, Krieg PA. Overexpression of the tinman-related genes XNkx-2.5 and XNkx-2.3 in Xenopus embryos results in myocardial hyperplasia. Development 1996;122:3549-56.

66. Cooper AF, Yu KP, Brueckner M, et al. Cardiac and CNS defects in a mouse with targeted disruption of suppressor of fused. Development 2005;132:4407-17.

67. Lyons I, Parsons LM, Hartley L, et al. Myogenic and morphogenetic defects in the heart tubes of murine embryos lacking the homeo box gene Nkx2-5. Genes Dev 1995;9:1654-66.

68. Goddeeris MM, Schwartz R, Klingensmith J, Meyers EN. Independent requirements for Hedgehog signaling by both the anterior heart field and neural crest cells for outflow tract development. Development 2007;134:1593-604.

69. Washington Smoak I, Byrd NA, Abu-Issa R, et al. Sonic hedgehog is required for cardiac outflow tract and neural crest cell development. Dev Biol 2005;283:357-72.

70. Goddeeris MM, Rho S, Petiet A, et al. Intracardiac septation requires hedgehog-dependent cellular contributions from outside the heart. Development 2008;135:1887-95.

71. Liang Q, Wiese RJ, Bueno OF, Dai YS, Markham BE, Molkentin JD. The transcription factor GATA4 is activated by extracellular signal-regulated kinase 1- and 2-mediated phosphorylation of serine 105 in cardiomyocytes. Mol Cell Biol 2001;21:7460-9.